Electrochemical CO_2 reduction in membrane-electrode assemblies

Ge, Lei; Rabiee, Hesamoddin; Li, Mengran; Subramanian, Siddhartha; Zheng, Yao; Lee, Joong Hee; Burdyny, Thomas; Wang, H.

DOI
10.1016/j.chempr.2021.12.002

Publication date
2022

Document Version
Final published version

Published in
Chem

Chem

CellPress

Review

Electrochemical CO_2 reduction in membrane-electrode assemblies

Lei Ge,[1,2] Hesamoddin Rabiee,[1,2,3] Mengran Li,[2,4] Siddhartha Subramanian,[4] Yao Zheng,[5] Joong Hee Lee,[6] Thomas Burdyny,[4] and Hao Wang[1,*]

SUMMARY

Electrochemical conversion of gaseous CO_2 to value-added products and fuels is a promising approach to achieve net-zero CO_2 emission energy systems. Significant efforts have been achieved in the design and synthesis of highly active and selective electrocatalysts for this reaction and their reaction mechanism. To perform an efficient conversion and desired product selectivity in practical applications, we need an active, cost-effective, stable, and scalable electrolyzer design. Membrane-electrode assemblies (MEAs) can be an efficient solution to address the key challenges in the aqueous gas diffusion electrodes (GDE), e.g., ohmic resistances and complex reactor design. This review presents a critical overview of recent advances in experimental design and simulation of MEAs for CO_2 reduction reaction, including the shortcomings and remedial strategies. In the last section, the remaining challenges and future research opportunities are suggested to support the advancement of CO_2 electrochemical technologies.

INTRODUCTION

The availability and affordability of fossil fuels are the key issues for society in the present and future. Using fossil fuels also causes carbon emission problems. There is an increasingly urgent need to decouple carbon emissions from economic activity without stifling growth.[1–4] Electrochemical technologies for producing essential global commodities, such as chemicals, liquid fuels, and fertilizers, from gases such as CO_2, CH_4, or N_2 are emerging as clean and viable processes that could compete economically with fossil fuel-driven processes (Figure 1).[5,6] Attractive characteristics of electrochemical processes include modular designs, near-ambient operating pressures and temperatures, and the potential to integrate electrocatalytic processes with electricity from renewable sources (e.g., wind and solar). These attributes could enable less-centralized and more sustainable manufacturing industries decoupled from fossil fuels combustion and potentially provide efficient and versatile platforms to store renewable energy in chemicals, H_2, or hydrocarbon fuels.[7] These electrochemical conversions could be profitable in locations with an abundant supply of renewable energy (e.g., Northern Europe, which has an oversupply of renewable energy at times) and markets for chemical products.

Electrochemical reduction of CO_2 to chemical feedstocks has particular attractions.[8–13] On the one hand, it reduces the amount of CO_2 being released to the atmosphere, complementing other CO_2 emission reduction strategies such as CO_2 capture and storage;[14] on the other hand, the electrochemical CO_2 reduction reaction (CO_2RR) produces a variety of essential chemicals that used to be

The bigger picture

CO_2 electrochemical reduction reaction (CO_2RR) enables conversion of greenhouse gas CO_2 into value-added products, which simultaneously reduces carbon emissions and reduces the usage of fossil fuels as feed materials to produce fuel/chemical products. It also provides the potential to integrate electrocatalytic processes with electricity from renewable sources for storing renewable energy. Membrane-electrode assemblies (MEAs) can be an efficient solution to address the key issues in aqueous electrolyzer design and enable the industrial scale-up. In this paper, we reviewed recent advances in the experimental design and simulation of MEAs. The discussion of existing challenges and future research priorities for guiding MEA development and understanding reaction mechanism is also provided.

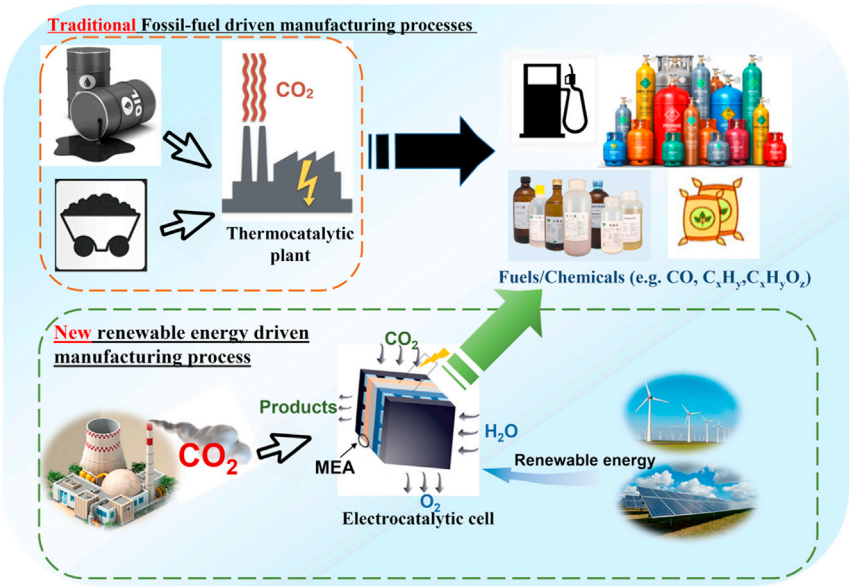

Figure 1. Schematic of fossil-fuel driven chemical manufacturing process and sustainable fuel/chemical production from CO_2 electrocatalysis

from petroleum, including CO (e.g., producing many liquid hydrocarbons via Fischer-Tropsch process), formate, methanol, methane, and other longer chain hydrocarbons.

In the typical electrolysis cell, CO_2 is reduced at the cathode, and water is oxidized at the anode. The cathode and the anode chamber are typically separated by a separator or polymeric ion exchange membrane (e.g., Nafion).[15] Catholytes choices can be aqueous solutions of inorganic salts (e.g., $KHCO_3$),[16] ionic liquids (e.g., 1-ethyl-3-methylimidazolium tetrafluoroborate),[17] and organic solvents (e.g., acetonitrile).[18] The main reaction for focus in the electrolysis cell is the cathode CO_2RR, CO_2 reduction mainly occurs within a gas-liquid-solid triple-phase reaction boundary. The energy efficiency is insufficient to be economically competitive, due to the limited mass transfer, product selectivity and high cell voltages at high rates, including high ohmic loss, and electrode overpotentials. An adequate supply of gas reactants to the catalyst surface becomes more crucial at higher current densities to maintain a high reaction rate. The selectivity of CO_2RR is highly dependent on catalyst materials and the triple-phase reaction microenvironment. Most of the current research focuses on catalyst material rather than mass transfer or microenvironment. In general, the CO_2 mass transportation is limited by its solubility in catholyte solutions. Meanwhile, the CO_2 mass-transport characteristics in membrane-electrode assembly (MEA) cells or gas diffusion electrode (GDE) cells are also influenced by the reactor configuration, electrode structure, catholyte selection, and operation conditions (e.g., pH, pressure, temperature).[19] These factors, in addition to catalyst materials, can have significant impacts on the reaction pathways because of their effects on the local concentrations of reactants and products. Often, the solubility and diffusion of CO_2 in the electrolyte limits the rate of CO_2 mass transfer and, thus, the overall reaction rate. The solubility can be increased by operating the electrochemical reactor at high pressure or switching to a more costly (and often more toxic or corrosive) solvent as the electrolyte,[20] but a more promising approach to overcome both CO_2 solubility and diffusion limitations is the GDE.

[1]Centre for Future Materials, University of Southern Queensland, Springfield Central, QLD 4300, Australia

[2]School of Chemical Engineering, The University of Queensland, Brisbane, QLD 4072, Australia

[3]Advanced Water Management Centre, Faculty of Engineering, Architecture and Information Technology, The University of Queensland, St. Lucia, QLD 4072, Australia

[4]Department of Chemical Engineering, Faculty of Applied Sciences, Delft University of Technology, van der Maasweg 9, 2629 HZ Delft, the Netherlands

[5]School of Chemical Engineering and Advanced Materials, The University of Adelaide, Adelaide, SA 5005, Australia

[6]Department of Nano Convergence Engineering, Jeonbuk National University, Jeonju-si, Jeollabuk-do 54896, Republic of Korea

*Correspondence: hao.wang@usq.edu.au

https://doi.org/10.1016/j.chempr.2021.12.002

The cathode in a CO_2RR electrolyzer provides (1) active catalyst sites; (2) provides contact interfaces between CO_2, electrolyte, and the solid catalyst; and conducts (3) electrons to the active catalyst sites. To tackle the mass transport and reaction rate limitation of the gaseous electrocatalytic reactions in the aqueous electrolytes, GDEs are proposed that can provide conjunction of a solid, liquid, and gaseous interface, the electrical conducting catalyst determines the electrochemical reaction between the liquid and the gaseous phase.[21,22] GDEs can be distinguished from the traditional simple planar or porous electrode by how CO_2 contacts with the electrolyte: with the planar or porous electrode CO_2 is dissolved in the bulk electrolyte, but, in the GDE, the gas diffuses through a porous gas-diffusion layer to the electrode/electrolyte interface. Reports in the literature suggest that GDE architectures can reduce the CO_2 diffusion path to the surface of the catalyst by up to 3-orders of magnitude, i.e., from ~50 μm on a planar electrode to around 50 nm in a GDE, which enables faster current densities.[23–25] Therefore, GDEs for electrochemical CO_2 reduction results in an order-of-magnitude increase in obtainable limiting current densities compared with planar non-GDE systems.[26–28] Despite this improvement, there are challenges in aqueous GDE systems, e.g., significant ohmic resistances from electrolyte layers and catalyst dissolution/delamination. These issues limit the further improvement of current densities at applied overpotentials and increase the reactor design complexity for industrial implementation.

MEAs, also known as "fuel cell-type," "zero-gap," "catholyte-free," or "gas-phase electrolysis,[29–31]" can be an efficient solution to address the challenges of the aqueous GDE. The MEA design for electrochemical cells has been widely used for fuel cells and water electrolyzers. A proton exchange membrane is typically used as an electrolyte in the MEAs, and gaseous reactants (e.g., CO_2) can be directly fed with no aqueous electrolyte between the electrodes. The mainstream of the catholyte is absent for the MEA, whereas the catalyst-membrane interface requires electrolytes to allow ion transport across the ion-exchange membranes. The reactions in the cathode and anode are similar to the non-MEA design. As for the main difference in the MEA design (Figure 2), the GDE and the ion-exchange membrane (e.g., Nafion) are attached as solid catholyte; in such case, gas/liquid products are collected in the feed side, and the flowing catholyte between the catalyst layer (CL) and ion-exchange membrane can be eliminated. Therefore, this membrane-based fabrication method can greatly reduce ohmic resistance and improve current density. Through modeling study, the MEA can reduce the ohmic loss from the catholyte when producing CO at high current density operation.[32] By utilizing MEA cells in CO_2RR, high current densities upward of 100 mA cm^2 have been achieved, which are an order of magnitude higher than using typical aqueous architectures.[33–35]

For the GDEs systems and the associated electrocatalysts, there are extensive material-centric reviews published in recent years. These reviews and prospects have enriched our fundamental understanding of the catalytic mechanism, catalytic pathways, product selectivity, and control factors in these processes.[19,21,36–41] Herein, we present this critical review on MEAs and their recent advances for CO_2RR application. It covers the material selection and design, mass transfer mechanisms in MEAs, and system design. The experimental findings in recent advances in MEA systems for CO2RR present the summary of design MEAs with improved activity (e.g., current density) and selectivity (e.g., faradic efficiency of targeted product). The review of modeling methods in design and performance of MEA via modeling provides the fundamental understanding of reaction mechanism and mass transfer in MEAs that contribute to the activity, selectivity, and stability in CO_2RR and engineering designs for practical applications. At the end of this review, the discussion of

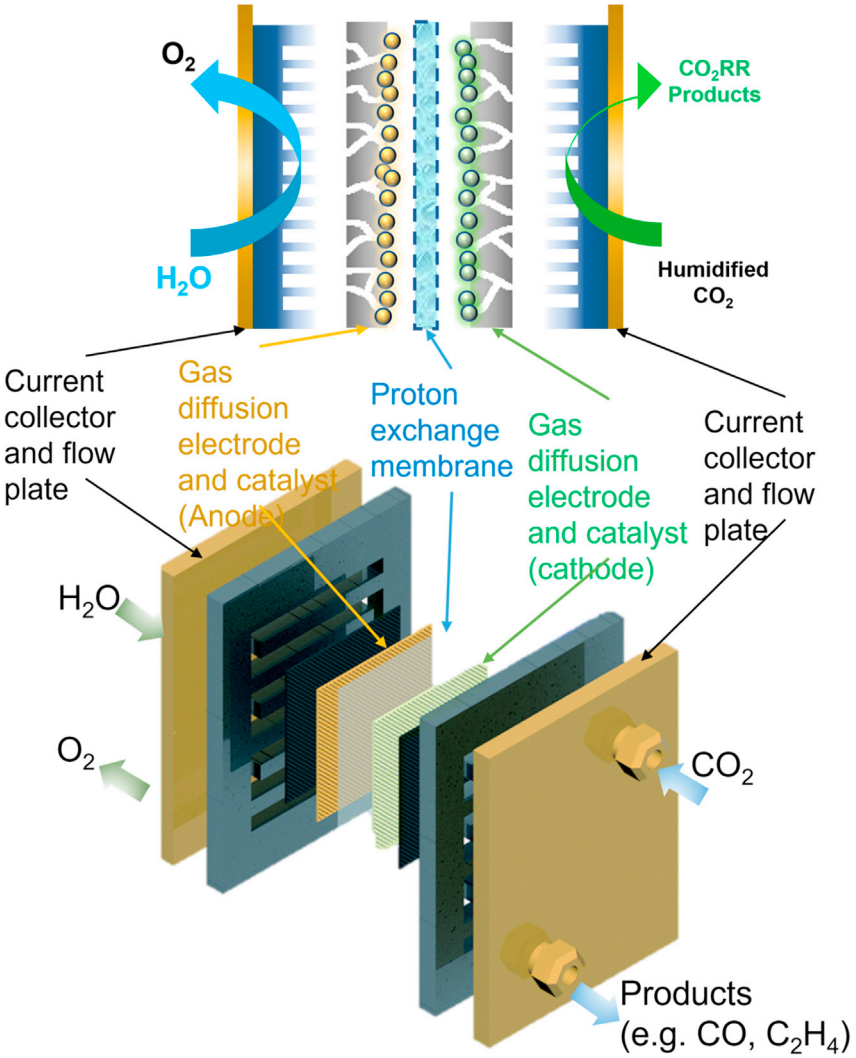

Figure 2. Schematic of membrane-electrode assembly for CO_2 electrocatalysis

existing challenges and future research priorities for guiding MEA development and understanding reaction mechanism is also included.

Recent advances in MEA systems for CO_2RR

The CO_2RR has been mostly tested in the aqueous phase, displaying the limitations of CO_2 solubility and ohmic resistance between catalysts and electrolytes. MEA CO_2RR electrolyzers offer several advantages, compared with systems with flowing-electrolyte; therefore, recently researchers have developed electrolyte-free systems for efficient CO_2RR.[32,42–59] It has been reported that MEA (or zero-gap or fuel cell-like) systems show a lower resistance and cell potential due to the absence of electrolytes. In addition, pumping an electrolyte brings some complexities to the systems (e.g., pumping, purification of electrolyte, etc.), whereas electrolyte-free systems have ease of scalability and operation without any possible catalyst poisoning from the impurities of the electrolyte.[19] Besides, other issues such as electrolyte consumption by CO_2 and GDE flooding are effectively eliminated. Another important advantage of MEA reactors is their superior product and voltage stability as well as energy efficiency compared with electrolyte-flowing systems.

MEA-type electrolyzers have not been extensively studied for multicarbon products and the formation of these products via more complex reactions requires more studies.[60] Gabardo et al. used MEA electrolyzer to produce concentrated multicarbon products at industrially relevant current densities, confirming the feasibility of using MEA-type reactors to produce liquid products with high concentration.[43] They prepared the MEA via sputtering of Cu onto a porous polytetrafluoroethylene (PTFE) membrane. By running the reactor at a slightly elevated temperature (40°C), they achieved cathode outlet concentrations of ~30% ethylene and the direct production of ~4 wt % ethanol with over 100 h stability.[43] Recently, Gu et al. used Cu catalysts with stepped sites with high surface coverages of *CO intermediates and the bridge-bound *CO adsorption, and it allowed to trigger CO_2 reduction pathways toward the formation of alcohols.[61] In this study, electrochemical deposition of Cu under a CO-rich environment led to the fabrication of defective Cu surfaces via stabilizing the surface energy, and the defect-site-rich surfaces greatly enhance the CO_2-to-alcohol reduction pathway. Using this defect-site-rich Cu catalyst, ~70% FE toward C_{2+} alcohols with partial current densities of >100 mA cm^{-2} was achieved.

In contrast to scarce multicarbon production on MEA-type electrolyzers, CO production has been one of the main targets of studies. Production of CO by using CO-selective Au and Ag electrocatalysts has been the main application of MEA systems for CO_2RR.[42,45,46,48–53,62,63] Yin et al. recently reported a current density of 0.5 A cm^{-2} (at 3.0 V cell voltage) with over 85% FE for CO with an MEA reactor, shown in Figure 3A.[31] Using CEMs results in an acidic environment on the cathode side, causing a severe hydrogen evolution reaction (HER), thereby, they used an alkaline ion-exchange membrane. As can be seen in Figure 3B, CO_2RR occurs on Au (as the CO-selective electrocatalyst), deposited on an alkaline polymer electrolyte membrane coupled with oxygen reduction in the anode (IrO_2) with pure water. The FE of CO reached 95% at cell voltages of 2–2.4 V and 85% at a cell voltage of 3 V where current density exceeded 500 mA cm^{-2} (Figure 3C). One advantage of the zero-gap design is that the operating temperature of the reactor can be easily controlled and adjusted throughout the cell. The operating temperature of MEA CO_2RR is of great importance and it was observed that cell voltage decreases with temperature (cell voltage decreases from 2.5 at 30°C to 2.2 V at 80°C, Figure 3D). However, increasing temperature also causes a reduction in FE of CO. The main reason for cell voltage decreases at higher temperatures was due to better ionic conduction (less resistance as seen in Figure 3E) and improvement in the reaction kinetics at higher temperatures. When increasing the temperature facilitates of both CO production and H_2 evolution at the same time, however, due to the greater activation energy of HER on Au catalyst (i.e., CO_2RR is favorable over HER on Au), HER benefits more than CO, and, therefore, FE of HER increases lead to a lower FE of CO. The temperature of 50°C–60°C was found to be the optimal temperature to keep FE of CO over 90% and cell voltage less than 2.3 V.

MEA CO_2RR electrolyzers can also be designed for liquid products. Recently, several studies have attempted to produce concentrated formic acid by using formate-selective electrocatalysts such as Sn, Bi, and In,[29,55,56,64–66] including a modified all-solid-state MEA electrolyzer that produced formic acid solutions of up to nearly 100 wt %.[67,68] In this modified design, humidified N_2 gas was purged through a solid-state electrolyte (SSE) (instead of a liquid electrolyte) in the middle chamber to collect formic acid vapor through the anion exchange membrane (AEM) (Figure 4A). The concept of employing an SSE was inspired by the ion-conducting solid polymers or ceramics in the battery for more stable and electrolyte-free production

of liquid products, such as formic acid. SSE helps to transport electrogenerated cations or anions (protons or formates in the case of HCOOH) to form pure products, avoiding mixture with dissolved solutes (such as the commonly used $KHCO_3$) in the case of a conventional liquid electrolyte. In this design, SSE is either an anion or cation conductor. Depending on the type of solid ion-conducting electrolyte in between, the HCOOH product could be formed via the ionic recombination of crossed ions at either the left (H^+ conductor) or right ($HCOO^-$ conductor) interface between the middle channel and membrane and diffuse away through the liquid water (Figure 4A). A high concentration of formic acid can be obtained by a simple cold-condensation process, while the N_2 stream can go back to the reactor. 2D A bi-based electrocatalyst (Figure 4B) is used because of the high formate selectivity and reaction rate of nanosheets with large catalytic active surface area. In addition, CO_2RR is coupled with a hydrogen oxidation reaction at the anode chamber, and, therefore, no liquid electrolyte is used, benefiting the practical applications of this design. The main advantage of this design is that no by-products are produced ($CO_2 + H_2 \rightarrow HCOOH$). Using this design with 2D Bi as electrocatalyst at cell voltages as low as 1.1 V resulted in formate FE of over 80% and current density over 200 mA cm^{-2} (Figure 4C);[68] therefore, formic acid with purities as high as 12 M was achieved, which is far higher than the high-rate electrolyte-based designs.[66,69]

To further improve the performance of formate formation in the all-solid-state design, grain boundary-rich Bi was used (Figure 5A) as the electrocatalyst, leading to over 90% FE of formate (Figure 5B) and formate purity of 14.8 M or 63 wt %. Furthermore, formate purity was improved to nearly 100 wt % via using dry N_2 (Figure 5C), which minimized water vapor involvement in the final product. Moreover, in this design, the cathode GDL is completely separated from liquid media by the N_2 passing section, which solved the flooding issue and can guarantee its stability even when operated under large negative overpotentials for high catalytic currents. Such high concentrations of formic acid can be directly used for formic acid fuel cells.[70] Similar studies are required for other liquid products of CO_2RR, such as alcohols. In general, employing MEA reactors to generate products rather than CO and formic acid are rare,[43,59] and much attention is needed to optimize MEA systems for various products.

AEM has been used successfully for MEA CO_2RR and dealing with the issue of severe HER when cation exchange membranes (CEMs) are used.[71,72] However, the crossover of CO_3^{2-}/HCO_3^- species (produced from CO_2 neutralization) or anion products (such as formate) through the AEM limit their long-term performance.[44,73–77] In addition, the carbonation of CO_2 on the cathode surface causes unstable CO_2RR operation. This issue considerably decreases CO_2 utilization in the reactor and leads to an overestimation of catalytic performance.[44,76] In a study for CO_2RR to ethylene, it was estimated that CO_2 loss due to crossover is three times larger than CO_2 conversion.[59] In addition, CO_2 is emitted together with O_2 in the anode chamber; therefore, it necessitates an additional gas separation. Yin et al. estimated that, if the ratio of CO_2 flow rate to CO_2 consumption rate is less than 10, transfer of CO_3^{2-}/HCO_3^- species into the anode side is negligible and the main charge carrier is OH^-.[31] However, the large-scale application of MEA CO_2RR with AEMs is still impeded by the product crossover and their mechanical and chemical stability.[72,78]

To solve the issue of crossover, Ozden et al. proposed a cascade reactor coupling a solid-oxide CO_2-to-CO electrochemical cell (SOEC) at 800°C with a CO-to-product (such as C_2H_4) MEA,[79] as shown in Figure 6A. By doing this, carbonate/bicarbonate formation from CO_2 and crossover to the anode side are eliminated and 110 h stable

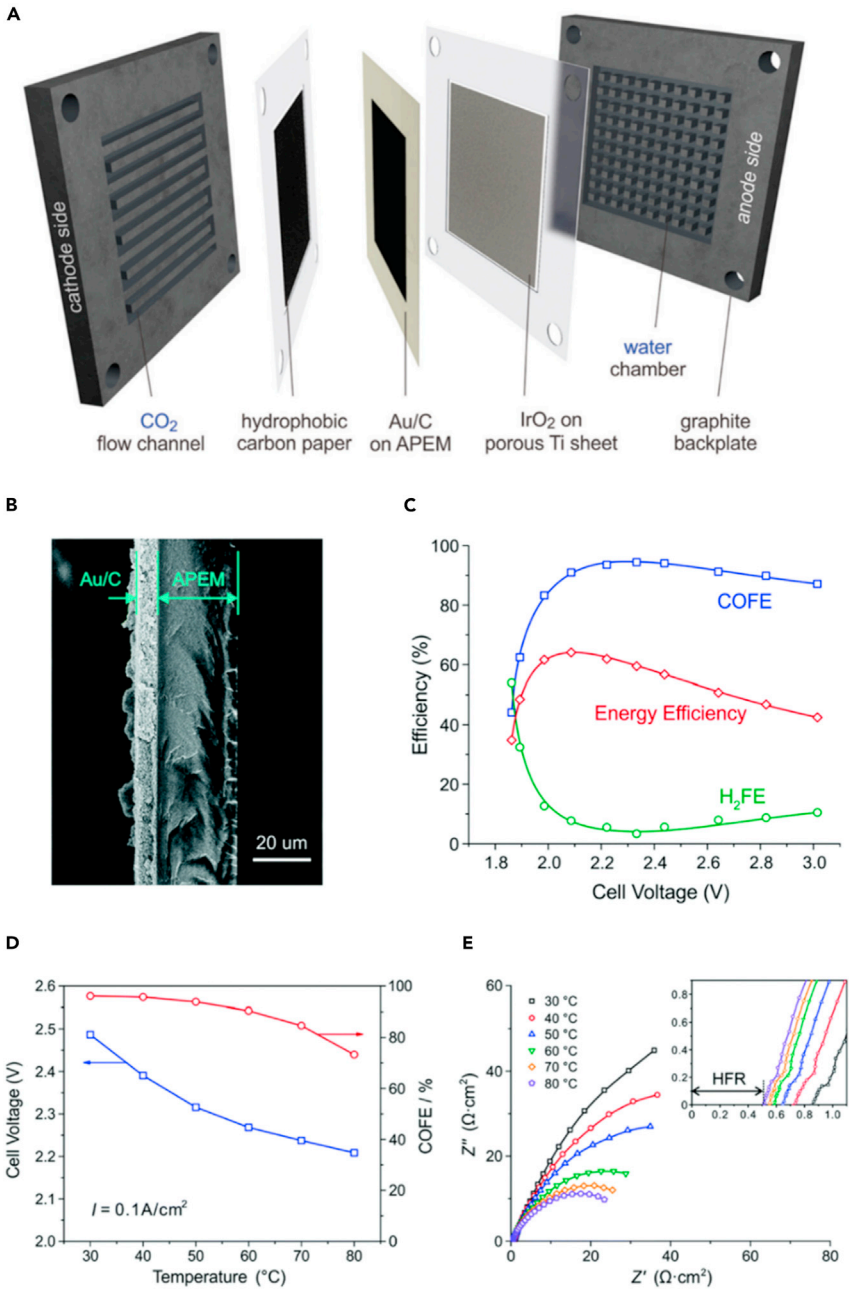

Figure 3. Features of a MEA electrolyzer and CO_2RR performance

(A) Structural illustration of CO_2 electrolyzer with dry CO_2 in the cathode and pure water in the anode.

(B) A cross-section SEM image of catalyst layer deposited on alkaline polymer exchange membrane; (C) Cell performance CO_2 electrolyzer as a function of cell voltage.

(D) The effect of operating temperature on cell voltage and FE of CO in an MEA CO_2RR electrolyzer.

(E) The impedance spectra recorded at open-circuit voltage, the inset magnifies the high-frequency region to show the change of ionic conduction with temperature. Reproduced with permission.[31] Copyright 2019, The Royal Society of Chemistry.

operation with an ethylene energy efficiency of >25% was achieved. The success of this design depends on performing CO-to-ethylene in MEA with the energy efficiency well beyond the performances in the literature. The authors designed a

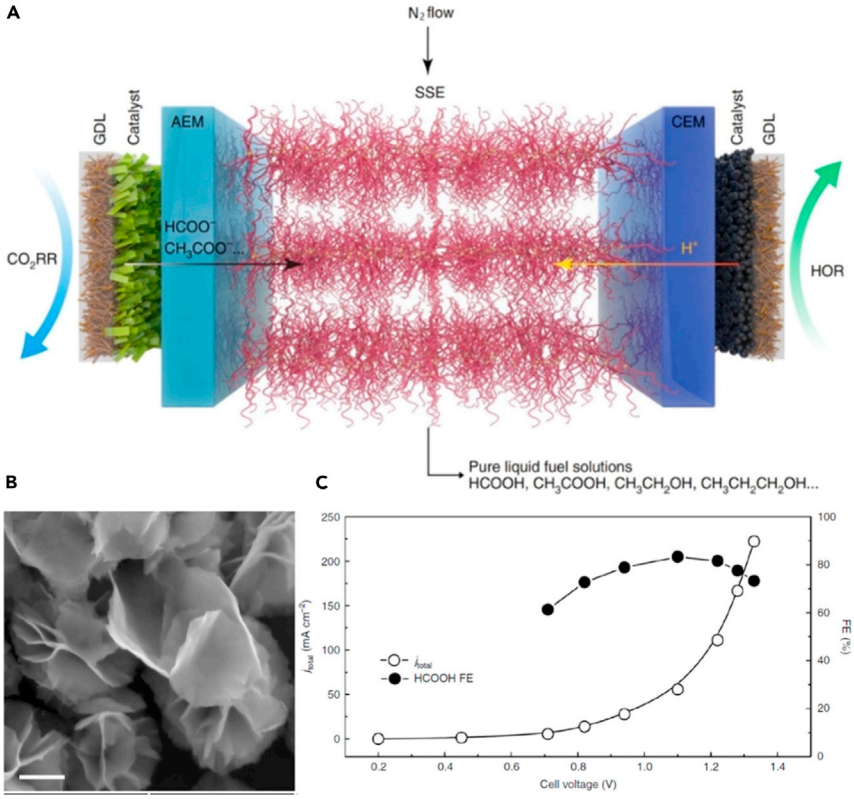

Figure 4. Using solid electrolyte and CO_2RR performance

(A) Schematic illustration of modified all-solid MEA CO_2RR electrolyzer, SSE, the generated pure formate vapor was brought out from the middle solid electrolyte using 100 sccm humified N_2.

(B) TEM of Bi-based nanosheets used as the electrocatalyst.

(C) The current densities and the corresponding formate FEs against cell voltages on a 2D-Bi all-solid-state cell, The generated pure HCOOH vapor was brought out from the middle solid electrolyte using 100 sccm humified N_2. Reproduced with permission.[69] Copyright 2019, Springer Nature.

layered catalyst structure composed of a metallic Cu, N-tolyl-tetrahydro-bipyridine, and SSC ionomer (Aquivion D79-25BS) (shown in Figure 6B) to achieve a high-rate and efficient CO-to-C_2H_4 conversion in an MEA electrolyzer. In this design, N-tolyl-tetrahydro-bipyridine improves the stabilization of key reaction intermediates, and SSC ionomer enhances CO transport to the Cu surface, enabling a C_2H_4 FE of 65% at 150 mA cm^{-2}, as shown in Figure 6C with 110 h stable operation. The cascade design required 138 GJ per ton of ethylene, which was less than what was required for the one-step MEA (267 GJ per ton of ethylene). Furthermore, the performance was enhanced by switching oxygen evolution in the anode to glucose oxidation reaction. Due to the 1 V less thermodynamic potential of glucose oxidation as compared with oxygen evolution reaction (OER), this led to reducing the total energy requirement to 89 GJ per ton of ethylene.[79]

Dealing with CO_2 crossover, recently Sargent et al. proposed conducting CO_2RR in an acidic environment (1 M H_3PO_4) and using a proton-exchange membrane (PEM).[80] They noticed that the addition of K^+ cations reduces the FE of HER and leads to an increase of FE other desired products, and this shift correlates with the concentration of K^+, as can be seen in Figure 7A. The presence of K^+ in the vicinity of the catalyst active sites can accelerate CO_2 activation and result in efficient

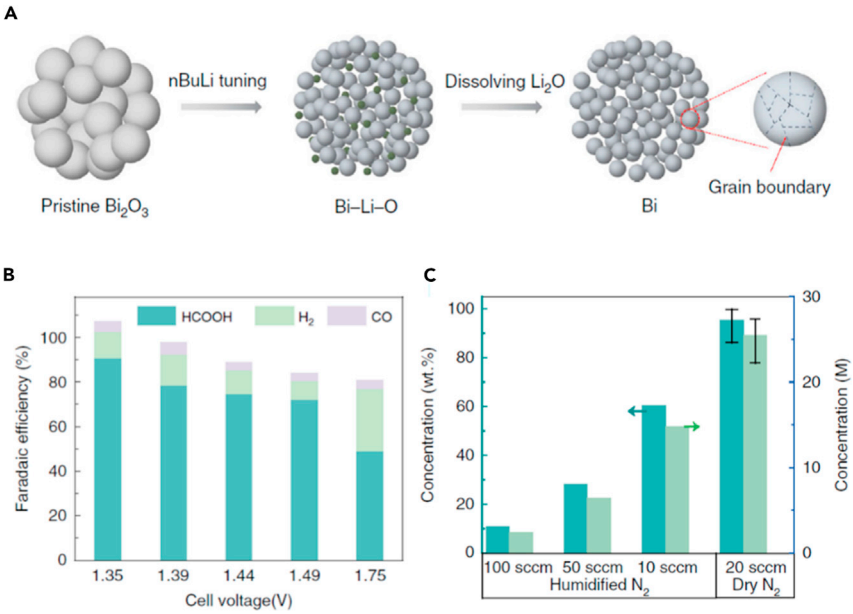

Figure 5. Catalyst design in a all-solid-state electrolyser and CO_2RR performance

(A) Schematic illustration of the fabrication process of grain boundary-rich Bi electrocatalyst.

(B) The corresponding FEs of formic acid vapor under different cell voltages on an all-solid-state cell with grain boundary-rich Bi electrocatalyst.

(C) Dependence of formic acid product concentration on the N_2 gas flow rate under a fixed overall current density of 200 mA cm^{-2}. By utilizing dry N_2 gas flow, up to nearly 100 wt % pure formic acid was achieved. Reproduced with permission.[68] Copyright 2020, Springer Nature.

CO_2RR. Consequently, a single-pass CO_2 utilization of 77% was achieved for performing CO_2RR at pH < 1 on Cu, although this number is usually less than 2% for both alkaline and neutral reactors due to CO_2 crossover.[80] The modeling of pH on the cathode surface at different current densities and distances from the cathode showed that at current densities well above 200 mA cm^{-2} the pH of the cathode surface is neutral/alkaline, even if the bulk pH was acidic (Figure 7B). This is due to the high consumption rate of local protons that exceeds the mass transport of protons from the bulk. Therefore, as seen in Figure 7C, when current density goes higher than 200 mA cm^{-2}, the formation of methane was observed due to locally alkaline conditions. However, even at current densities as high as 1 A cm^{-2}, pH decreases to 6.3 within 33 μm of the electrode (Figure 7B), assuring that any locally generated carbonate would be converted back to CO_2 for ensuring reduction. One drawback of this method is limited K^+ solubility in low pH solutions. To deal with this issue, the authors used a cation-augmenting layer (CAL) to enrich K^+ at the Cu surface, as shown in Figure 7D. This layer was a cationic perfluorosulfonic acid (PFSA) ionomer composed of tetrafluoroethylene and sulfonyl fluoride vinyl ether. The acidic $–SO_3H$ group is expected to exchange its protons with K^+ from the bulk electrolyte in a non-acidic local environment, sustaining a high K^+ concentration at the catalyst surface (Figure 7D). The CAL allows cation (e.g., H^+ and K^+) transport in the direction from electrolyte to catalyst surface while slowing OH^- diffusion out, leading to higher surface pH, which was reported to facilitate C–C coupling.[35]

The carbonate migration can also result in the degradation of the anode materials, recently highlighted by Vass et al.[81] Their results based on 0.1 M aqueous anolyte (KOH, $KHCO_3$, CsOH, and $CsHCO_3$) have shown that the local pH at the anode-membrane is predetermined by the ions produced from electrolysis and the passage

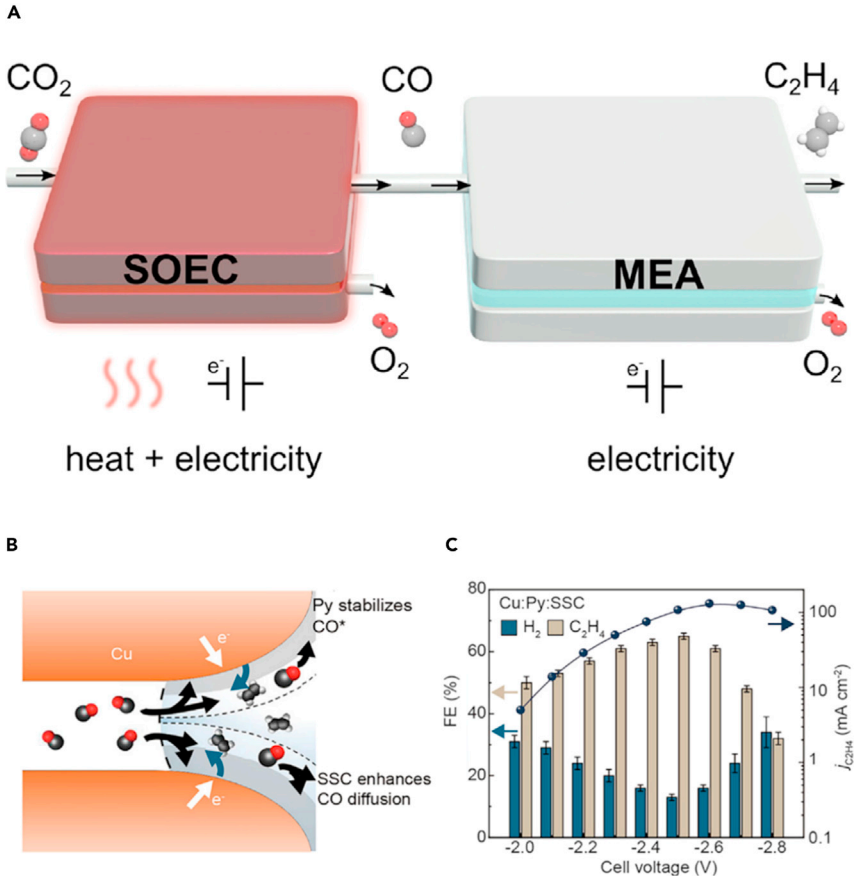

Figure 6. Cascade reactor for CO_2 crossover issue

(A) A schematic illustration of renewable CO_2-synthesized C_2H_4 in a combined system consisting of a CO_2-to-CO SOEC and a CO-to-C_2H_4 MEA.

(B) Introducing additives to improve CO diffusion and stabilize CO* intermediates.

(C) Enhanced C_2H_4 selectivity performance on the cascade reactor with the modified electrocatalyst. Reproduced with permission.[80] Copyright 2021, Elsevier.

of ions through the membrane, instead of by bulk anolyte solutions. The authors found that the local pH decreased continuously at the anode-membrane interfaces when the cell was fed with alkaline anolyte due to the migration of carbonate. Such acidified interface caused dissolution of Ni and precipitation of $NiCO_3$ at the membrane, which caused significant degradation of the cell performance. Interestingly, they also demonstrated that the use of a pH-neutral bicarbonate aqueous solution can minimize carbonate transport and, thus, slow down anode degradation of Ir-based anodes. This work also highlights the importance of considering both the electrodes and membrane in designing a stable and reactive MEA for CO_2 electrolysis.

Another option to mitigate the issue of crossover is using a bipolar membrane (BPM, composed of a CEM and AEM) in which cations are rejected by AEM and anions are rejected by CEM.[82] Thereby, no ion can pass a BPM except the ions generated or combined at the PEM/AEM interface. However, it has been reported that zero-gap electrolyzers with a BPM have a very low FE of CO, and the reason remains unclear, probably due to the difficulty of monitoring local pH.[83] Yan et al. recently designed a bipolar membrane with ~50-nm-thick weak-acid layer to control and

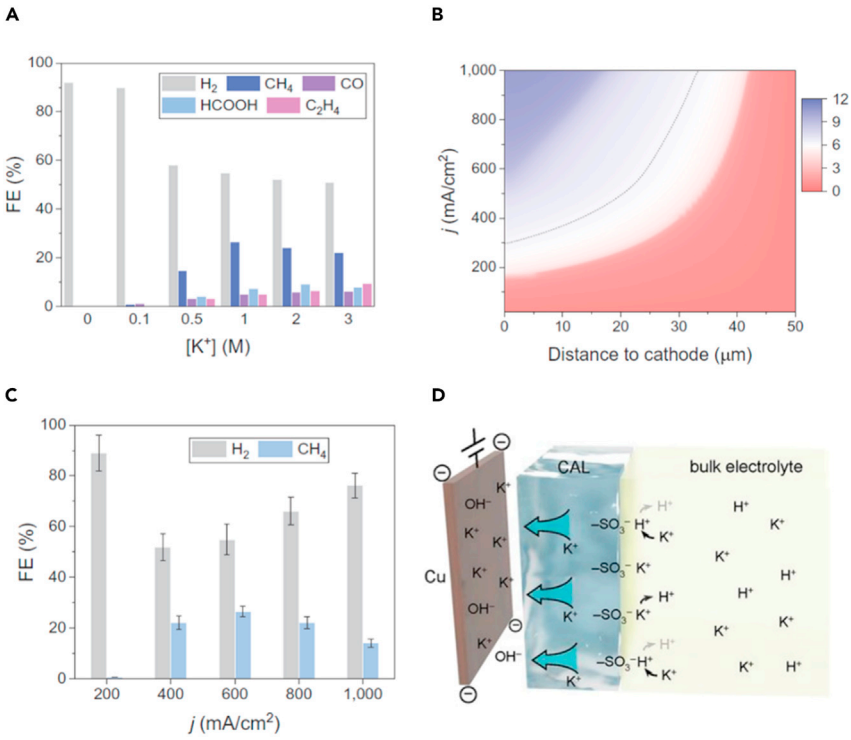

Figure 7. Role of K^+ to CO_2 crossover and performance

(A) FE toward all products on sputtered Cu catalyst in 1 M H_3PO_4 with different KCl concentrations at 400 mA cm^{-2}.

(B) Modeling of pH at different distances to the cathode and current density in 1 M H_3PO_4 and 3 M KCl.

(C) FE toward H_2 and CH_4 on sputtered Cu catalyst at different current densities in 1 M H3PO4 and 3 M KCl.

(D) Schematic illustration of ionic environment and transport near the catalyst surface functionalized by the PFSA ionomer. Reproduced with permission.[81] Copyright 2021, Springer Nature.

monitor local pH and ultimately suppress hydrogen evolution.[63] They added 10 layers of polyanion/polycation on the CEM part of a BPM and observed a significant increase in FE of CO along with local pH (Figure 8A). Therefore, the added layer acted similar to a weak-acid cation exchanger and suppressed HER.

In addition to the importance of the ion-exchange membrane and the issue of products crossover, MEA can be flooded if the water transported from the anode side is more than the water needed for CO_2RR on the cathode side (around 5 mg $cm^{-2}h^{-1}$). Flooding can be possibly managed by tuning GDE hydrophobicity to adjust MEA hydration, water uptake, and thickness of the AEM (water uptake is related to ion exchange capacity).[85] If AEM uptake is high, a lower amount of water transfers to the cathodic section of the MEA electrolyzer, however, AEM is more prone to swelling.[84] As can be seen in Figure 8B, AEM with a high water uptake membrane (HWUM) shows better stability in terms of FE of CO, as compared with AEM with low water uptake membrane (LWUM) when current density increases.[85] Another method of managing hydration is controlling cathode GDE hydrophobicity via increasing PTFE content as a water-repellency agent. As can be seen in Figure 8C, GDE prepared by a higher percentage of PTFE (29%) shows significantly higher FE of CO compared with the GDE with 6% PTFE when current density increases to

200 mA cm^{-2}. Finally, if AEM thickness increases, its water uptake capability substantially increases. Thereby, it was observed that thicker AEMs showed less stability at high current densities compared with thinner AEMs, as seen in Figure 8D. Through tuning these three factors, flooding can be avoided within an MEA; however, sufficient hydration of an MEA is necessary to facilitate anion transport through the cathode GDE. Shafaque et al. recently reported that by using humidified CO_2 feed, water uptake of a CEM increased 11%, resulting in 30% less energy demand compared with dry CO_2 feed due to enhanced ionic transport.[86] Similarly, using water vapor in the anode side, instead of water, which causes flooding, or operating CO_2RR at slightly elevated temperatures to enhance ionic conductivity and ionomer hydration properties of AEM.[87]

Apart from the flooding issue, MEA systems with an AEM are also prone to the formation of carbonate salts from CO_2 at high current densities and locally alkaline conditions.[54] This is similar to carbonation on GDEs during CO_2RR with liquid electrolytes.[21,87] Carbonation leads to the blockage of CO_2 transport, reduces reaction efficiency, and causes unstable CO_2RR operation. Xu et al. recently proposed a self-cleaning strategy to mitigate the formation of carbonate salts via cycling between continuous and altering operation modes, as shown in Figure 9A. Under the altering mode, a regenerative cell voltage, lower than the operational CO_2RR cell voltage, is applied to allow carbonate ions to migrate to the anode, lowering cathode concentrations and avoiding the formation of damaging salts. The regenerative cell voltage (−2.0 V) was set to lower the reaction rate to nearly 0 mA cm^{-2}, preventing further hydroxide/carbonate generation but maintaining a sufficiently negative polarization at the cathode to transport carbonate ions (Figure 9A).[54] During the regeneration step, carbonate salts move toward the anode via electromigration and, therefore, hinder the formation of carbonate salts at the cathode. Simulations showed that during CO_2RR in continuous mode at the voltage of −3.8 V, local carbonate concentration reached the potassium carbonate solubility limit within 1,200 s; therefore, carbonation is highly expected to occur after this point.[54] However, after 60 s of operation, carbonate concentration was well below the potassium carbonate solubility limit. This confirmed the effect of operating time on the accumulation of carbonations salts. Subsequently, applying a regeneration period of 30 s reduced lowered the carbonate concentration by 2,000-fold, indicating the effectiveness of this method to remove over 99.9% of carbonate at the cathode.[54] Compared with continuous operation with 10 h stability before a performance drop due to carbonation (Figure 9B), the alternating mode exhibited similar product selectivity with much higher stability for 236 h of operation (Figure 9C).

Efficient MEA-type CO_2RR with AEMs usually use an alkaline anolyte,[44,47,88,89] although the importance of the anolyte type on CO_2RR performance is not comprehensively understood. If the anode catalyst functions in either alkaline or pure water, MEA-type performance with an AEM should be independent of the anolyte medium. However, it was recently discovered that the cation crossover from anode to cathode side was a major contributor to the high performance of MEA electrolyzers with an AEM.[90] This crossover however causes cathode GDE precipitation due to the reaction between the unintended cations, CO_2, and the electrogenerated OH^-. The precipitation was found to be deep inside the GDE, blocking CO_2 pathways. Although rinsing the GDE with water has been proposed in the literature,[91] this cannot fully restore the cell performance due to the deep penetration of deposits, [47] unless rising is done with excessive pressure, which can be damaging to the structure of the gas diffusion layer.[87] Another solution can be increasing the humidity of the CO_2 feed stream, which, however, changes the overall operation of cell.[85] On the other

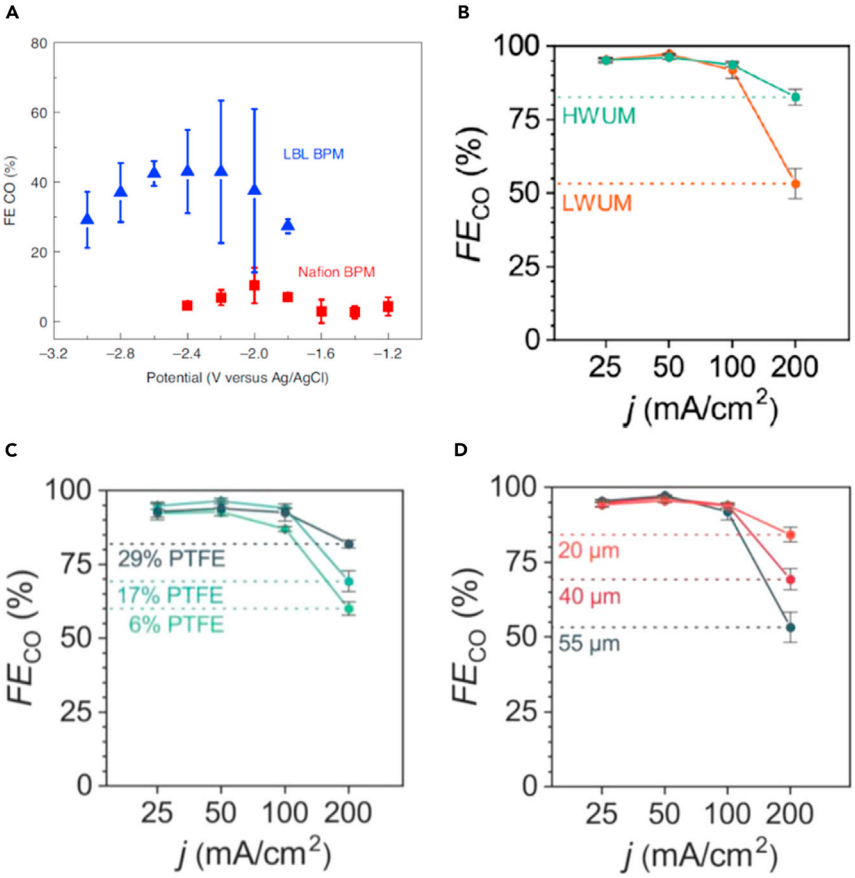

Figure 8. Strategies for crossover issues

(A) Comparison of an MEA electrolyzer performance between a BPM with Nafion CEM and a BPM modified via layer-by-layer in terms of FE of CO as a function of cathode potential.[64]

(B) Stability of FE of CO for AEM with HWUM and LWUM as a function of current density.

(C) Effect of PTFE content of a cathode GDE on FE of CO in an MEA electrolyzer.

(D) Effect of AEM thickness on FE of CO in an MEA electrolyzer. Reproduced with permission.[84] Copyright 2020, American Chemical Society.

hand, using pure water as the anolyte led to a drop in the current density to one-third due to the higher total charge transfer resistance compared with when KOH solution is used as the anolyte.

Therefore, a method to take advantage of alkaline anolyte and hinder precipitation can turn this challenge into an opportunity. Endrődi et al. recently proposed a method to use pure water as anolyte coupled with activating the cathode GDE by periodically infusing the cathode with different alkali cation-containing solutions.[90] With this method, an alkaline solution (e.g., 0.5 M KOH) is periodically fed to the cathode GDE to boost CO_2RR via the system design shown in Figure 10A, while pure water is used as the anolyte. This activation strategy led to a 3-fold increase in the CO formation rate (Figure 10B), indicating the success of this method. One important feature of this strategy is tailoring the solvent mixture based on the wettability of the GDE. Because the solution is delivered to the back of the GDE (through the hydrophobic gas-diffusion layer), the mixture containing alcohol (e.g., isopropyl alcohol) shows a lower contact angle (Figure 10C); therefore, it can penetrate through the GDE and reach the catalyst. It was seen that if alcohol was not used in the alkaline solution, the increase of CO production rate is much less

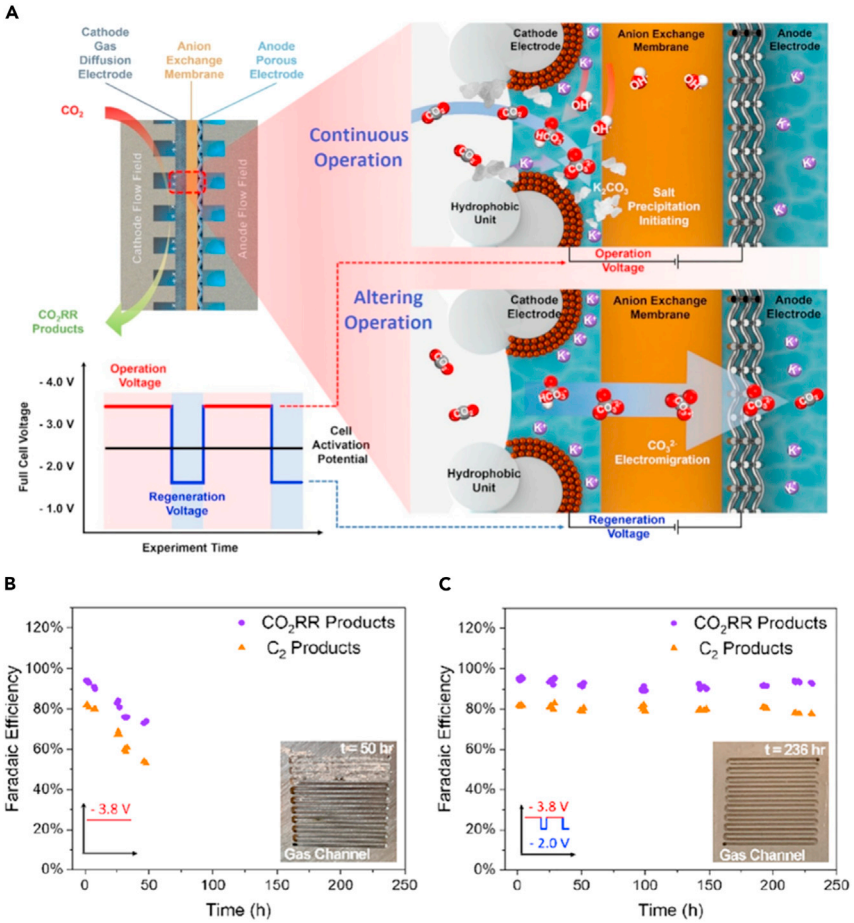

Figure 9. A self-cleaning strategy to mitigate carbonate formation

(A) Schematic of MEA CO_2RR electrolyzer and CO_2 conversion to bicarbonate and carbonate during continuous operation and altering operation with regeneration voltage. During the regeneration voltage of the altering mode, carbonate migration occurs through AEM to mitigate carbonation.

(B) Selectivity of the continuously operated system at −3.8 V during long-term operation.

(C) Selectivity of alternating operation sample (60 s at an operational voltage of −3.8 V and 30 s at regeneration voltage of −2.0 V) during long-term operation. Reproduced with permission.[54] Copyright 2021, American Chemical Society.

compared with when alcohol was added.[90] It is because the solution without alcohol penetrated only through the cracks of the hydrophobic gas-diffusion layer that it also results in a large variance in CO production. Overall, as can be seen in Figure 10D, the results of activation via KOH infusion and water anolyte were identical to when KOH was used as the anolyte (red solid line and blue dash line), confirming the success of this process. Furthermore, this method showed acceptable performance for running long term and dosing KOH every 12 h, thus, as can be seen in Figure 10E, the current density of CO remained high over a 10 days run.

Another important feature of an MEA system is the cell voltage, as reducing the cell voltage directly results in increasing the energy efficiency and lowering the energy input.[92] Salvatore et al. analyzed the source of voltage loss in MEA systems with AEM, BPM (Figure 11A), and hybrid AEM (Figure 11B, where there is catholyte in the cathode side but the anode side is electrolyte-free). The source of voltage loss can be attributed

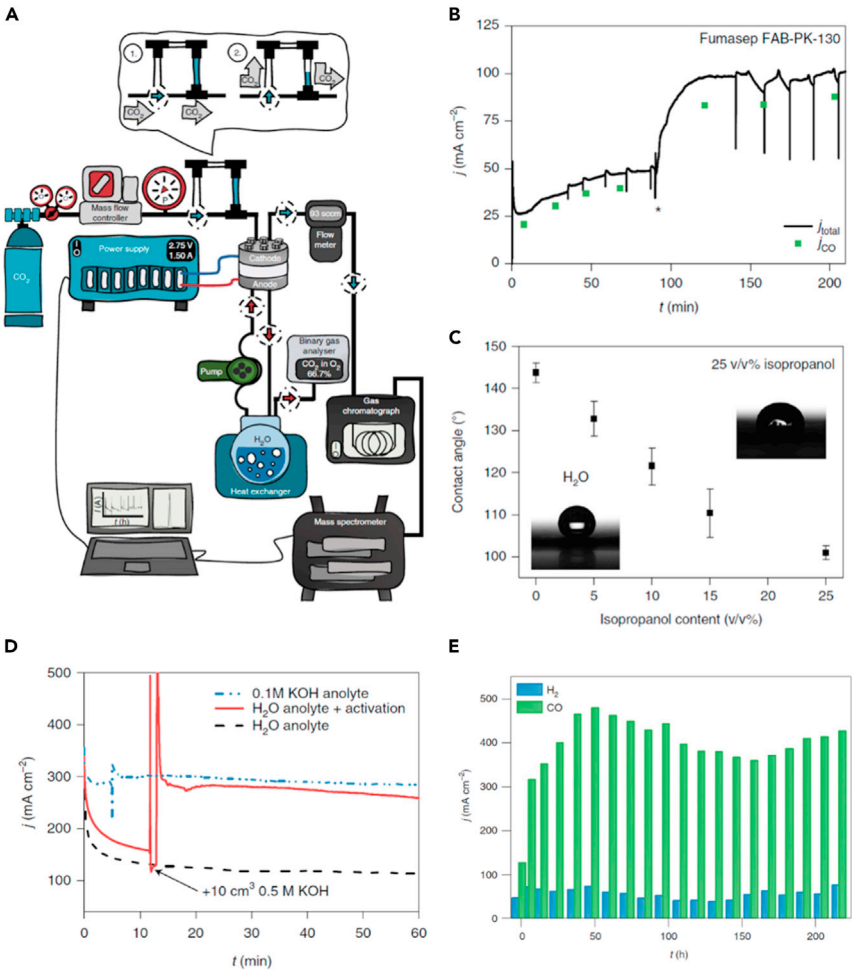

Figure 10. Infusion of alkali cation-containing solutions

(A) Schematic of the test framework employed to activate cathode GDE in an MEA-type system via KHO infusion. In the inset (top), "1" shows the continuous gas path to the cell and bypassing the activation loop. In position "2," the gas is driven through the activation loop, carrying the activation fluid into the cell.

(B) Chronoamperometric curves and CO partial current densities ($T_{cathode}$ = 60°C, 12.5 cm^3 cm^{-2} min^{-1} CO_2 feed rate, pure water anolyte) measured using Fumasep FAB-PK-130 AEM.

(C) Contact angles of different water/isopropanol solvent mixtures on the microporous side of a gas-diffusion layer.

(D) Chronoamperometric curves before and after activating the cathode GDE with 10 cm^3 of 0.5 M KOH solution in 1:3 isopropanol/water mixture.

(E) CO and H_2 partial current during constant-voltage electrolysis (ΔU = 3.2 V, T = 60°C water anolyte, 12.5 cm^3 cm^{-2} min^{-1} feed rate). The cathode was activated with 5 cm^3 of 1 M CsOH solution in a 1:3 isopropanol/water mixture after every 12 h of the electrolysis. Reproduced with permission.[91] Copyright 2021, Springer Nature.

to the voltage drop in the anode, cathode, and membrane surface. Their results showed that at different current densities from 25 to 200 mA cm^{-2}, the MEA system with an AEM performed better compared with other configurations. Increasing the current density from 25 to 200 mA cm^{-2} led to 0.68 V increase in the cell voltage for the system with AEM, whereas, for the MEA with BPM and the hybrid system, this figure was 1.6 and 2.45 V, respectively. Specifically for the case of the BPM system, the voltage drop due to the membranes was significantly higher than others, which is due to the free energy required to auto associate water with the BPM.[93] In addition, for the hybrid system, the

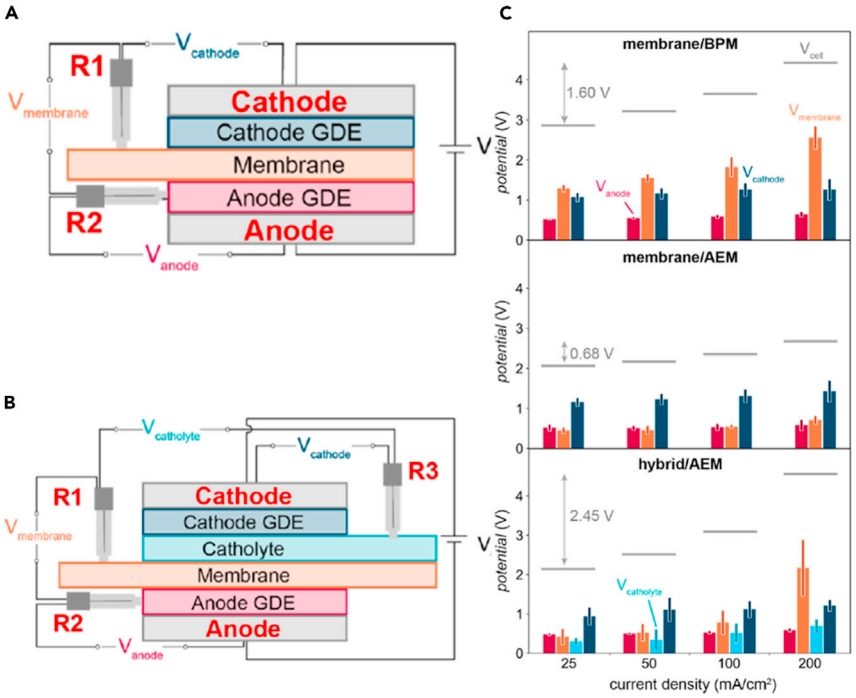

Figure 11. Voltage loss in MEA systems

(A and B) Schematic of voltage drop in (A) MEA system and (B) hybrid system with catholyte.

(C) Voltage measurements for the membrane/BPM, membrane/AEM, and hybrid/AEM flow cells at 25, 50, 100, and 200 mA cm^{-2}. The voltage for each component is labeled as follows: anode (red); membrane (orange); catholyte (blue; only relevant for the hybrid reactor); and cathode (navy). The full cell potential at each current density (gray horizontal lines) is the sum of all voltages measured for each component. Reproduced with permission.[93] Copyright 2019, American Chemical Society.

existence of a catholyte and the large interfacial resistance at the polymer/liquid interface contributed to an overall higher cell voltage required for the same current density (Figure 11C). Based on the analysis of voltages across the components, it can be concluded that the reactions at the anode and cathode are relatively efficient, and the membranes are responsible for much of the voltage loss. Therefore, this draws attention for a better understanding of membranes and the membrane-catalyst interface to lower the overall cell voltage and enhance the energy efficiency of an MEA system.[92]

Overall, the shortcomings of MEA-based electrolyzers for CO_2 reduction and the potential solutions are summarized in Table 1.

Design and performance of MEA via modeling

CO_2RR in MEA is a complex system. The performance of MEA is dependent on the contributions of many components, including cathode reaction, anode reaction, ion transportation in the membrane, and electrode-membrane interface exchanges. Many of those factors are interacting with each other. However, the experimental approach seems very limited to understand multiphase and ion transport phenomena inside the reactor at high current densities and how these influence the reaction kinetics and cell potentials. For example, the absence of liquid electrolyte at the cathode and the intimate cathode-membrane contact limits the use of reference electrodes to directly measure the cathode potential.[92] The electrode-membrane interface prevents straightforward understanding of the local reaction environment for the catalysts, such as the flow cells where a flowing catholyte is present. It is

Table 1. General shortcomings and remedies for MEA-based CO_2 electrolyzers

Shortcomings	Implications	Potential solutions	Ref.
Flooding	closure of CO_2 transfer pores	- adjusting GDE water uptake via ion-exchange capacity and GDE thickness - controlling cathode GDE hydrophobicity via PTFE content	Reyes et al. [85]
		- separating cathode GDE from - liquid media by a gas passing section	Fan et al.[67]
CO_2 crossover to the anode side	losing CO_2 in the cathode	- using a tandem design consisting of SOEC and MEA	Ozden et al.[79]
	re-emission of CO_2 with O_2 in the anode	- using acidic media with a CAL to enrich K^+ at the catalyst surface	Huang et al.[80]
Product concentration	necessitates a costly separation stage	using a carrier gas (such as N_2) to collect high-purity products	Xia et al.[68]
Carbonate formation on the cathode GDE	Blockage of CO_2 transport. Reducing reaction efficiency. Unstable CO_2RR operation.	considering a regenerative cell voltage, lower than the operational voltage to lower carbonate ions concentrations on the cathode and mitigate salt formation	Xu et al.[54]
Cation crossover from anode to cathode when using alkaline solution in anode	precipitation on the cathode GDE due to the reaction with crossover cation, CO_2, and electrogenerated OH^-	using pure water as anolyte and periodically infusing the cathode with alkali cation-containing solutions (e.g., 0.5 M KOH)	Endrődi et al.[90]
High voltage loss	reducing energy efficiency	designing no electrolyte cell, using AEM and improving membrane-catalyst interface	Salvatore and Berlinguette[92]

expected that the local environment should be affected by the ion-conducting nature of the membrane, the electrode activity and wettability, temperature, and the type of anolyte (e.g., $KHCO_3$, KOH, or pure water).[47,94,95] Similarly, the anode reaction (i.e., OER) will also be predetermined by the membranes, anolyte, anode catalyst materials, and the reactivity of cathode. For example, the AEMs and bipolar membranes in the reverse bias should allow the use of anodes based on transition metals (e.g., Ni, Co, and Fe), whereas the CEM or bipolar membrane in the forward bias requires the previous metal-based anodes such as IrO_2 or RuO_2, which are stable in an acidic environment. If pure water is used as the anolyte, a high flux of hydroxide ions is required from the cathode interface to the anode, which relies on the membrane properties (e.g., thickness and conductivity) and the cathode reactivity. On the other hand, the use of concentrated electrolytes such as aqueous KOH solutions could cause significant cation crossover to the cathode, and lead to the salt precipitation at the back of GDE and significant degradation of overall cell performance.

Multiphysics modeling could, therefore, shed light on multiphase transport phenomena, reaction kinetics, spatial effects, and thermal conditions within the cells, which is paramount to understand the underlying mechanisms and limitations of the MEAs. The modeling approach has been widely used to understand the multiphysics processes in electrochemical systems such as PEM fuel cells[96,97] and electrolysis systems.[98–100] There is an increasing number of modeling papers with a focus on the gas-diffusion electrode for CO_2 reduction in the presence of catholyte. The schematic shown in Figure 12 summarizes the approaches used by a few recent efforts to understand the mechanisms underlying the MEA processes based on anion-exchange membranes. To reduce the computation power, 1D model or a hybrid of

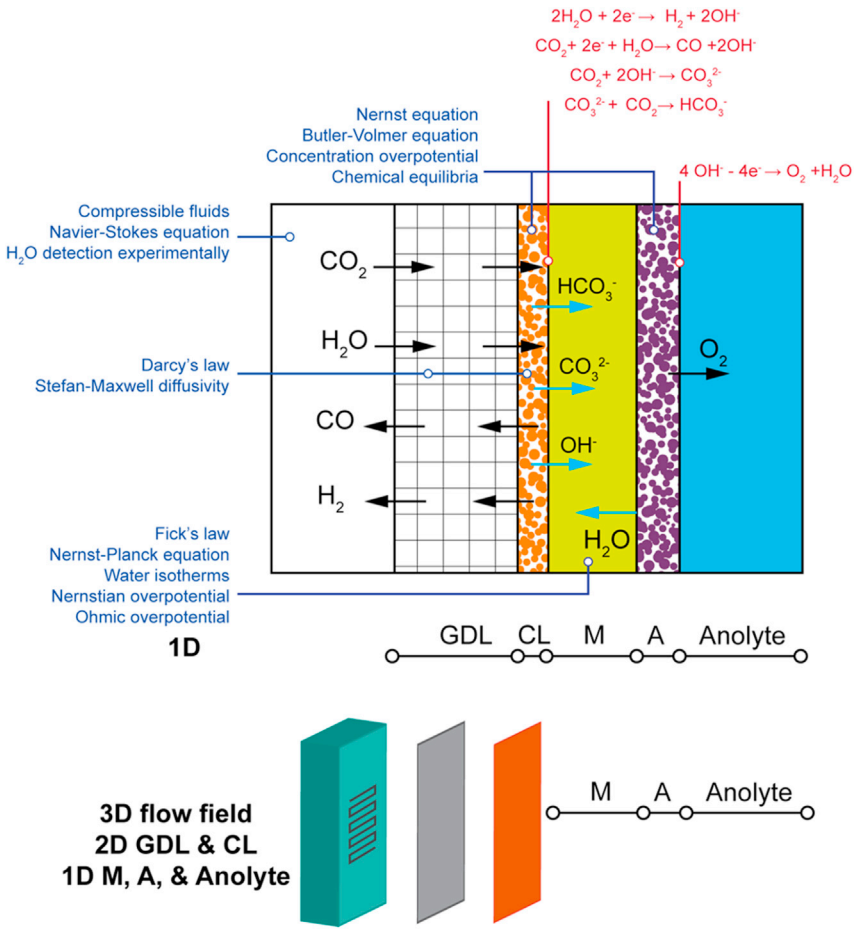

Figure 12. A schematic overview of the modeling approach to study the MEA cells, by using CO production as an example

3D/2D/1D models were commonly used for the MEAs usually with a focus only on the cathodes and membranes. Recent models are all derived from previous models on either PEM fuel cells or GDEs in the presence of catholyte, due to the similarities in mass transport of gases (as described by Stefan-Maxwell equation and Darcy's law), transfer of heat (associated with charge-transfer, chemical reactions, and joule heating), current-potential relations (as described by Bulter-Volmer, Nernst equation, concentration overpotential, and Nerstian overpotential), ion migration (e.g., Nernst Planck equations), water transport (e.g., electro-osmosis), and reactions (chemical reactions, electrochemical reactions, and chemical equilibria).[24,32,89,101]

Difference between MEA and the conventional GDE in the presence of catholyte

The intimate contact between electrode and membrane leads to some unique features. First, in the MEA setup with AEM, the CO_2 reduction occurs in an alkaline environment, whereas carbonate buffering and water dissociation reactions take place in ionomer and aqueous solutions at the electrode-membrane interfaces and could behave differently from in the bulk electrolytes depending on the hydration and ionic heads.[102,103] The carbonate-related reactions become more prominent in MEA and lead to significant CO_2 loss, which has been observed in the experimental studies.[44,47,49,69,73] Second, water management becomes crucial for MEA

operations. Dehydration of the membrane could take place for the full MEA without aqueous anolyte at high current densities due to the consumption of water during reactions and water evaporation.[32,104] In the presence of the anolyte (e.g., KOH or $KHCO_3$), precipitation of the potassium carbonate at the cathode side becomes a critical issue for long-term stability.[32,47] Third, the transport of ions and molecules in the membrane and ionomer should be significantly affected by molecular frictions and solute-solute interactions because of the limited water content inside the ionomers. This means that Stephan-Maxwell equation should be more suitable to describe the transport within ionomers than the Nernst-Plank equation, though it is more complicated and adds complexity to the numerical model.[32] As Weng, Bell, and Weber have provided detailed descriptions of the governing principles, equations, key assumptions, and boundary conditions in their numerical models of MEAs to produce carbon monoxide[32] and hydrocarbons,[105] we focus our vantage in this review on the findings from recent MEA modeling results, mainly based on Weng et al.'s,[32,105] Mccallum et al.'s,[101] and Wheeler et al.'s[89] modeling papers on AEM-MEA configuration, which has recently demonstrated great potential to achieve high selectivity and stability at high current densities, the CO_2 reduction occurs in an alkaline environment.

The modeling results reveal that the MEA-based configurations (including full MEA and exchange-MEA, see Figure 13A) have significantly lower cell voltage at 2.54 V by 44% than the conventional aqueous GDEs (4.54 V) to convert CO_2 to CO, as a result of the eliminated ohmic loss across the cathode and anode.[32] The KOH exchange-MEA requires less cell voltage compared with the full MEA and $KHCO_3$ exchange MEA, as shown in Figure 13B. The detailed cell voltage breakdown, as shown in Figure 13C, manifests that the reduction of the cell voltage over KOH exchange-MEA originates from the eliminated anode Nernstian potential, sufficient hydration of the membrane and ionomers, and improved thermodynamic potentials, with all these benefits bestowed by the supply of KOH electrolyte at the anode side.

Crossover of carbonate and liquid products

The model also predicts salt precipitation can occur at the cathode in the exchange-MEAs, a critical issue for MEA setups, (Figure 14) thanks to the inclusion of the carbonate buffer reactions and hydration estimation in the modeling. The authors pointed out that the K^+ ions are driven by chemical and electrical potential gradients to migrate from the anolyte to the cathode, form K_2CO_3 at the cathode side, and precipitates when it exceeds the solubility limit.[32]

The carbonate forms particularly at AEM-MEA because of the exposure of concentrated OH^- ions and a high local CO_2 concentration.[43,105] Again, the concentrated OH^- ions are the result of CO_2RR and HER and limited water at the cathode of the MEA. The carbonation is the main contributor to the observed significant CO_2 loss, because the carbonate species will cross the membrane to the anode and get oxidized to CO_2. Interestingly, the carbonate ions serve as the primary charge carriers across the electrodes at low current densities, whereas the transport of hydroxide ions only becomes more prominent at high current densities at 1 A cm^{-2} where OH^- production rate exceeds the buffering reaction rates (see Figure 14A).[32] The modeling results unveiled the essential but complex roles of local pH in the performance of the MEAs. A high local pH can minimize proton availability for the unwanted HER[105] but will increase CO_2 losses and lower CO_2 availability close to the catalyst surface (resulting in a high Nernstian overpotential).[107] Such trade-offs highlight the importance of the local buffering reactions to balance the pH effects.

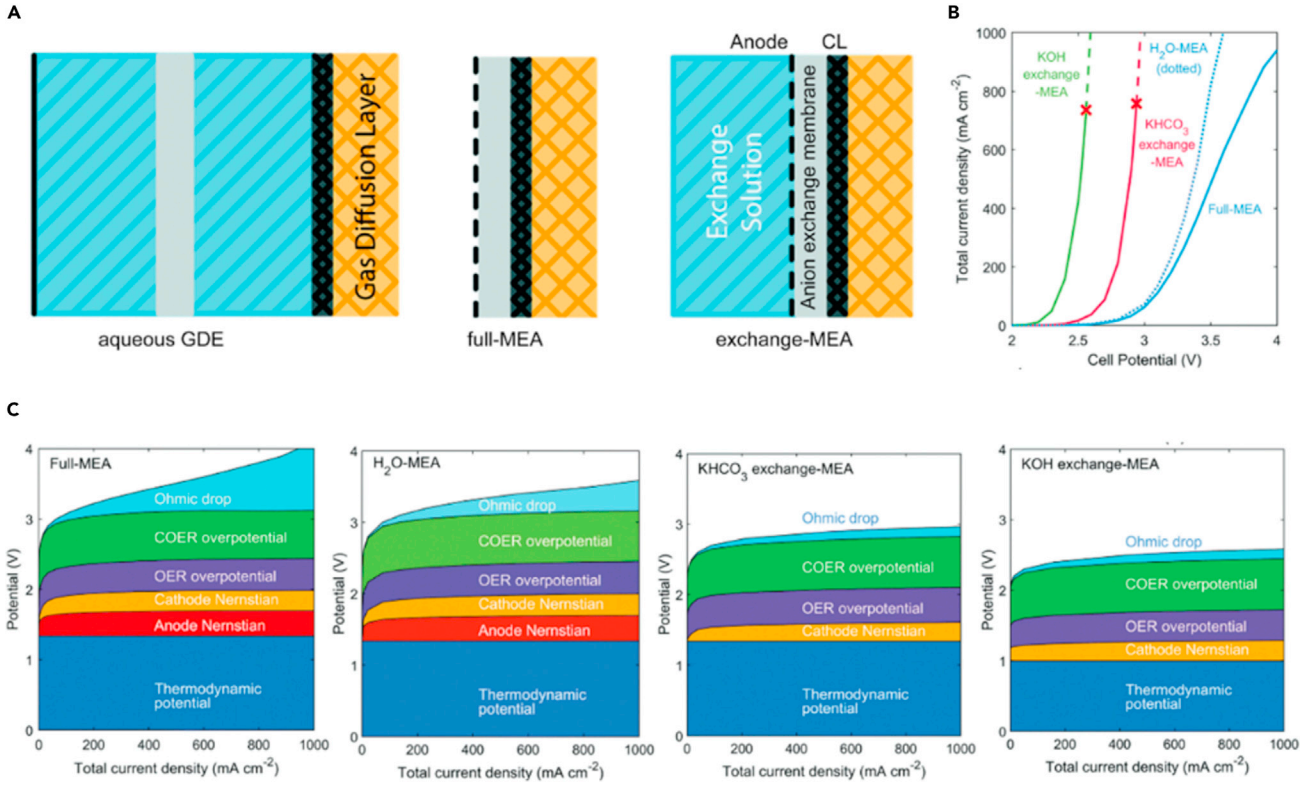

Figure 13. Modelling of full MEA and exchange-MEA

(A) Schematic illustration of the GDE in the presence of an aqueous electrolyte, full-MEA, and exchange-MEA.

(B) The total current densities of the full-MEA and exchange-MEAs as a function of the overall cell potentials.

(C) Cell potential breakdown for the full-MEA and exchange-MEA with anolyte as water, $KHCO_3$, and KOH aqueous solutions. Reproduced with permission.[102] Copyright 2019, The Royal Society of Chemistry.

McCallum et al.[101] recently applied the machine-learning technique to save computation power when modeling CO_2 electrolysis to produce ethylene and ethanol as the main product. In this report, they defined $\eta_{anion} = \int \frac{J_{HCO_3^-}}{\int OH^{-dx}}^{-dx+\int J_{CO_3^{2-}}^{2-dx}}$ as the matric to quantify carbonate crossover. The authors studied the changes of carbonate crossover by varying the CO_2 partial pressure, applied potential (or current densities), and membrane properties (i.e., membrane charges and thickness). Their modeling results showed that the carbonate crossover can be alleviated by (1) decreasing CO_2 partial pressure, (2) reducing membrane thickness, (3) increasing membrane charge, and (4) increasing current densities for positively charged membrane or reducing current densities for positively and neutral membranes (Figure 15). It is straightforward that lowering the CO_2 partial pressure can slow down the carbonation at the catalyst surface due to the lower CO_2 concentration. However, lower CO_2 concentration could also lead to degradation of product selectivity. A very recent report by Subramanian et al. unveiled, using a 3D model, that reducing the flow rate of the CO_2 feed can lead to spatial non-uniformity across the cathode.[108] Again, their 3D model was also modified with the experimentally measured CO_2 loss to the carbonates. From their model, they found that the CO_2 supply could be insufficient for the electrode area that is close to the effluent when the feed is at 10 sccm at 200 mA cm^{-2} over a silver-based electrode. McCallum et al. suggested a moderate level of CO_2 concentration is desired for CO_2 reduction. The membrane

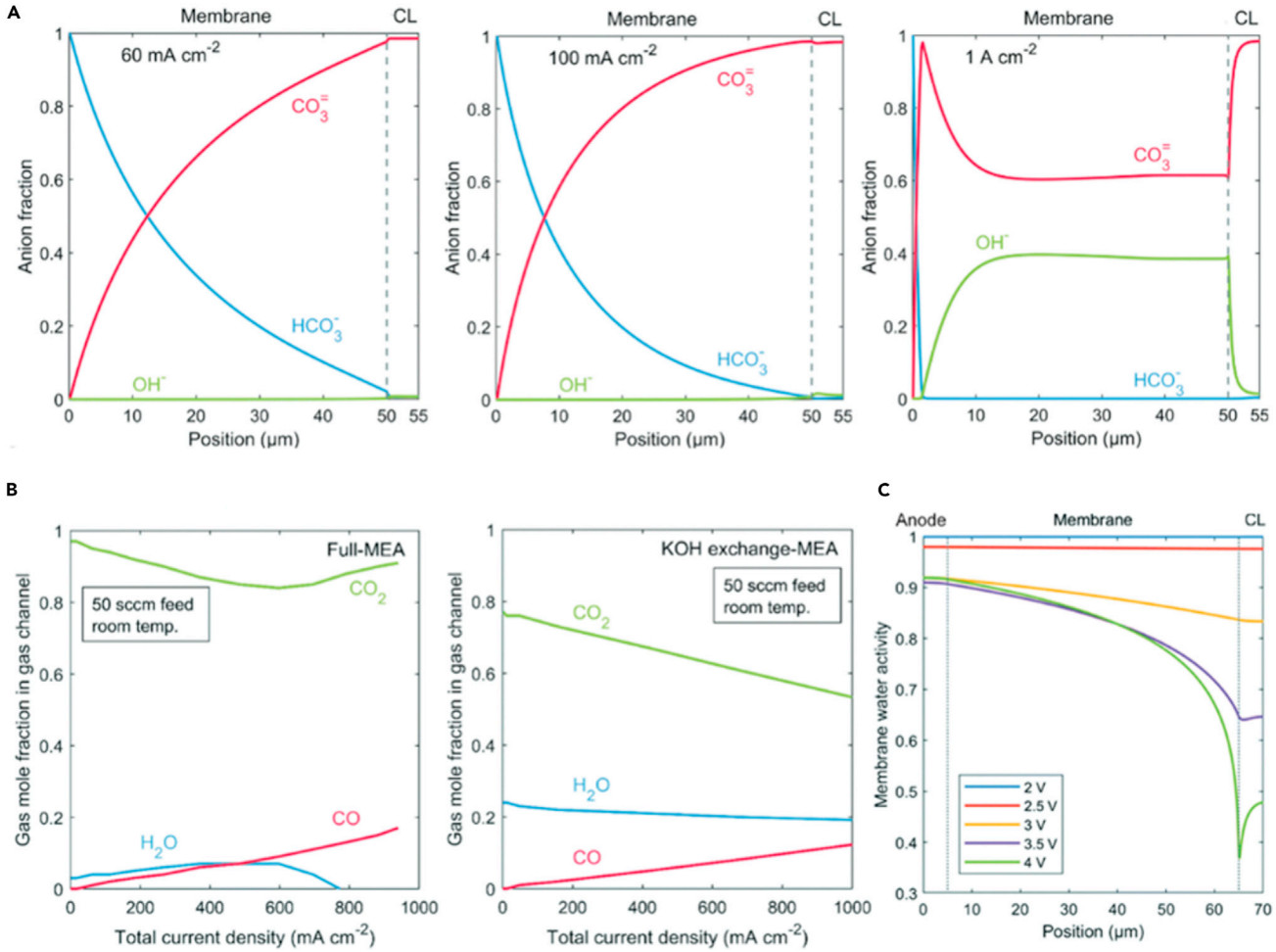

Figure 14. Modelling of salt precipitation in the exchange-MEAs

(A) The anion species as a function of position across the AEM and cathode catalyst layer.

(B) Gas mole fraction in the gas channel as a function of current densities for full-MEA and KOH exchange-MEA. Reproduced with permission.[102] Copyright 2019, The Royal Society of Chemistry.

(C) Water activity of the membrane as a function of position across the membrane and CL at varied cell potentials for Cu-based catalyst layer. Reproduced with permission.[106] Copyright 2020, The Royal Society of Chemistry.

properties determine the OH^- ion flux across the membrane, and a high OH^- flux could help reduce carbonate relative flux. For example, reducing the membrane thickness could allow shorter transport lengths for anions and a higher relative flux of OH^-, and, thus, minimize the carbonate crossover. What is more, a high AEM positive charge benefits the OH^- ion uptake and, thus, a reduced carbonate flux. When the membrane is a cation-exchange membrane, the carbonate crossover can also be reduced by the negative charge of the membrane, a large HCO_3^- gradient (if the anolyte is $KHCO_3$ aqueous solution) together with a large pH gradient.

A similar trend can be also observed for the CO_2 utilization (i.e., $\eta_{CO_2} = \frac{CO_2 electroreduction}{Total CO_2 consumption}$). A thin membrane and a low CO_2 partial pressure also benefit the reduction of Nerstian overpotential ($\eta_N = \frac{RT}{F} log \frac{c_{OH^-}}{c_{OH^-}}$ where C is the cathode and A is the anode) because it lowers the pH gradient across the cathode and anode (or a higher anode pH). This finding is consistent with Weng et al.'s report (Figure 14).

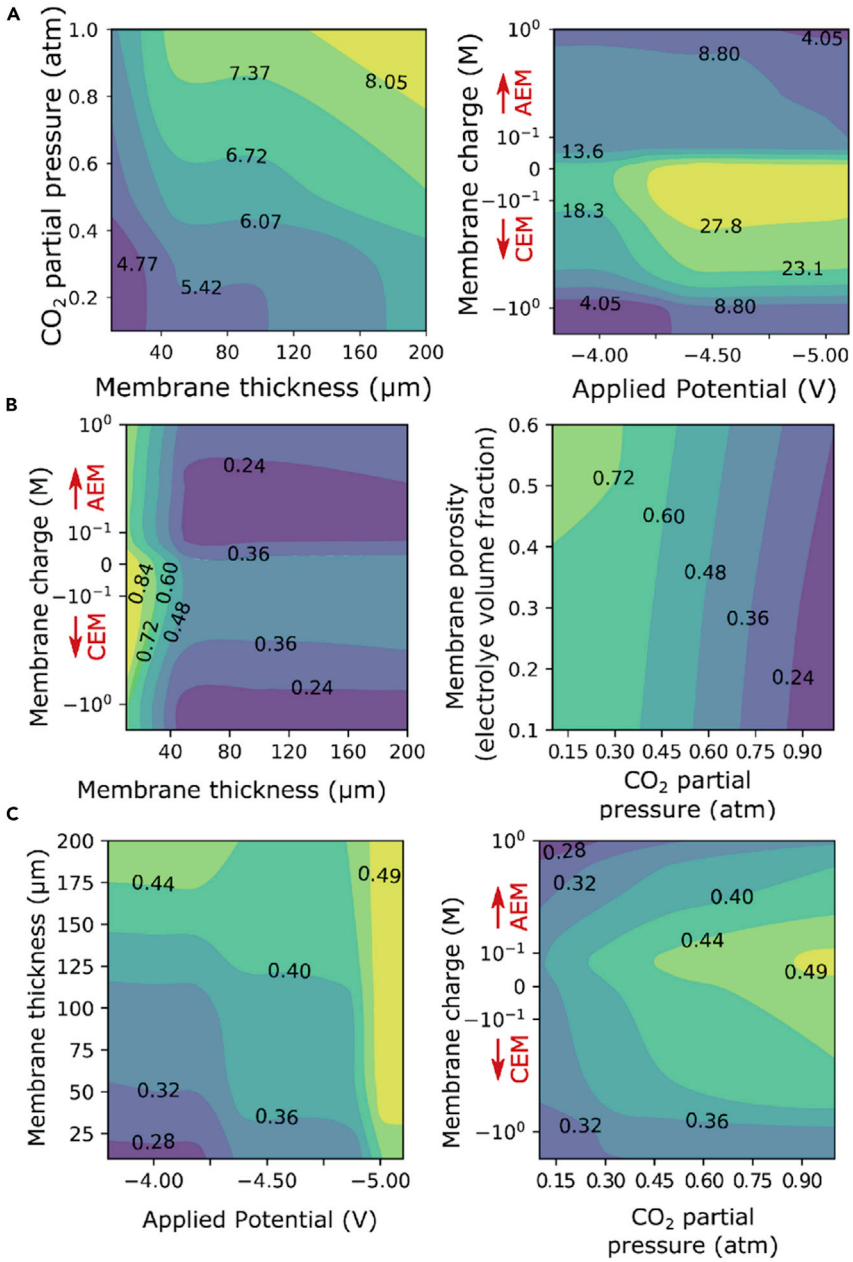

Figure 15. Operation parameters impact carbonate crossover

(A–C) The impacts of operating conditions or membrane properties on (A) anion, (B) CO_2 utilization, and (C) Nerstian overpotential. Reproduced with permission.[103] Copyright 2021, Elsevier.

Interestingly, their machine learning analysis over their previous work by Gabardo et al.[43] also suggested that the current densities and temperature are the two key factors affecting the crossover of ethanol product; a high current density and increasing temperature could help prevent ethanol crossover across the membrane.

Water management

As aforementioned, water management is crucial in the MEA-based electrolyzer and is determined by the reactor configuration, membrane properties, and operating

conditions, such as feed rates, current densities, and temperatures. As one of the main proton sources for CO_2 reduction, water can be quickly consumed at electrodes. Therefore, a high current density (or a high cell voltage) accelerates the dehydration process (Figure 14). Additionally, water evaporation from the ionomer may also take place. An elevated temperature induces a high water pressure but may also lead to evaporation if the relative humidity is low.[32] The dehydration process may disrupt the membrane ion conductivity, electrode local pH, and reaction kinetics, and consequently lead to degradation of CO_2RR reactivity and efficiency. In this case, the exchange-MEA could maintain better hydration of the membrane than the full MEA (Figure 14) whose hydration relies on the water vapor in the feed. On one hand, the dehydration process may disrupt the membrane ion conductivity, electrode local pH, and reaction kinetics and consequently lead to degradation of CO_2RR reactivity and efficiency. On the other hand, too much water transport could cause unwanted catalyst flooding at the cathode and block the gas diffusion to the catalyst surface. The water transport in the membrane is governed by the electro-osmosis process, which is defined as the movement of water associated with the movement of ions driven by an electric field through a membrane.[109] It is expected that a high gradient of chemical potential across the membrane or the ion flux could increase the water flux across the membrane. A high chemical potential gradient could be achieved by maintaining a high solution activity gradient or increasing the hydrostatic pressure. The electro-osmotic coefficient is a function of the membrane properties, the ionic characters, and the applied electric potential and remains underexplored through the experimental approach.

In a recent report, Wheeler et al.[89] quantified water transport in an exchange MEA CO_2 electrolyzer using humidity sensors integrated within the reactor and found that the water concentration at the catalyst-membrane interface remains constant, irrespective of humidity at the inlet feed (Figure 16). This means that more water will be drawn from the membrane to the cathode if the feed is dry. Significant water transport to the cathode from membrane likely promotes unwanted catalyst flooding, ion crossover, and salt precipitation. Such humidity data allowed the authors to build a semi-empirical model to describe the water flux from the membrane to the cathode. Their 3D model results are consistent with their experimental measurement. More importantly, the model results unveiled a more uniform distribution of water content in the flow field when the CO_2 is wet compared with the case where CO_2 is dry. Although the calculated water flux for both cases are similar, the different CO faraday efficiencies for these two cases highlight the important role of water distribution and source in the CO_2 conversion efficiency, rather than the availability of water, for the reactions.

We can conclude in this section that the multiphysics models are powerful to probe the transport and reaction mechanisms that cannot be easily measured in experiments. The model framework can be developed based on the existing models for PEM fuel cells and electrolyzers with some modifications to capture the unique features of the MEA setups in reactions, transport phenomena, and local environments. Experimental inputs such as humidity sensors at the flow field and the application of machine learning techniques are demonstrated to be useful to reduce the computation demand for complex 3D models. The modeling results could help clarify the contributions from polarization losses, species transport, membrane properties, and operating conditions such as current densities and gas feeds (CO_2 partial pressure and humidity). The modeling results unveiled several trade-offs, such as dehydration-cathode flooding and CO_2 loss—pH buffering, which present the challenges and opportunities to design high-performance MEAs.

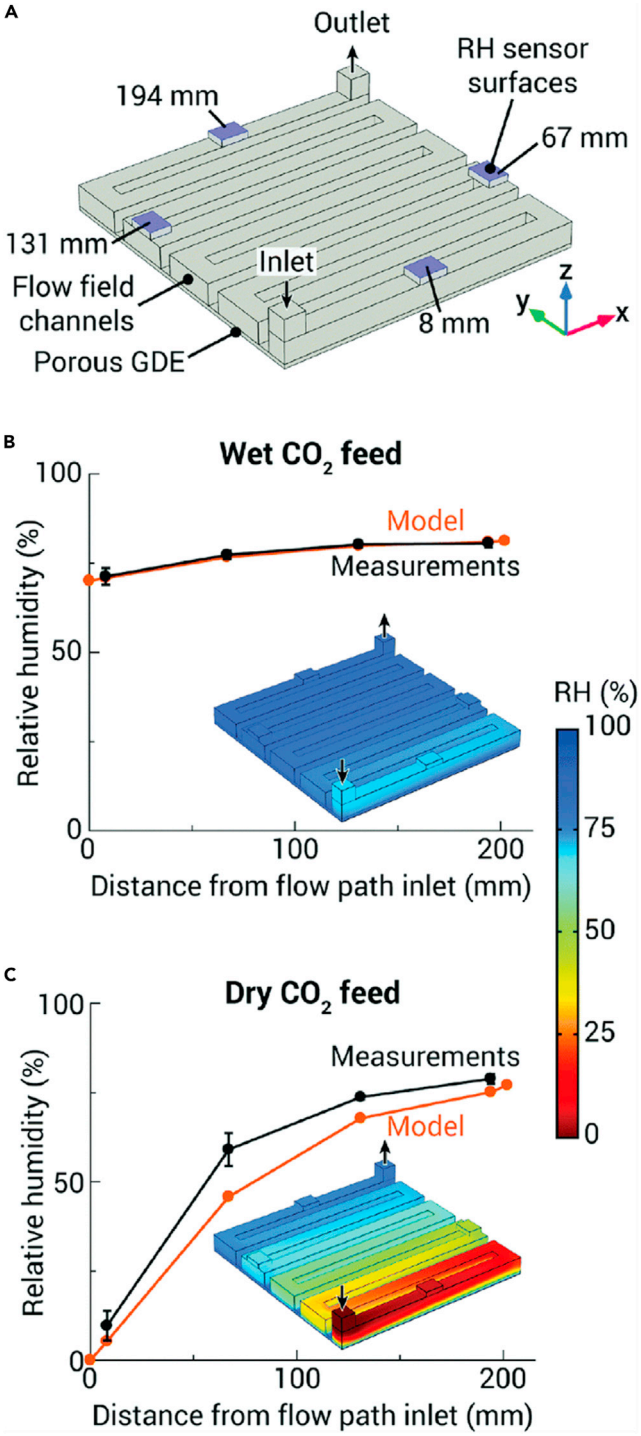

Figure 16. Modelling of water transport in an exchange MEA CO_2 electrolyzer

(A–D) (A) A schematic illustration of a 3D model of flow field mounted with humidity sensors, (B) relative humidity of the cathode flow field when the CO_2 feed is wet or (C) dry. The inset 3D model shows the distribution of relative humidity from the model at 100 sccm and 0 mA cm^{-2}. Reproduced with permission.[90] Copyright 2020, The Royal Society of Chemistry.

CONCLUSIONS AND PERSPECTIVES

In this review, we summarized the advances and challenges in designing MEAs for CO_2RR. Liquid-electrolyte systems have many intrinsic challenges, such as high ohmic resistance of the liquid electrolyte and flooding. MEAs consist of gaseous feeds at one or both electrodes and a solid ion-conducting polymer electrolyte between the electrodes, which can overcome the limitations of the aqueous GDE and ease the scale-up for industrial-scale electrolysis. The main challenges in industrial CO_2RR are related to energy efficiency (cell voltage, concentration overpotentials, and product selectivity) and current density (limited by mass transport). The energy efficiency determines the operation cost, and the current density affects the capital cost. Therefore, the MEA designs can reduce ohmic loss from catholyte and overall cell voltage, so the production selectivity can be maintained at a wider range of pH. Meanwhile, the operation of MEA at pressurized conditions can also benefit the current density and allow the direct usage of high-pressure industrial gas feeds. Meanwhile, similar to the MEAs in the fuel cells, the hydration management in MEA and the products/CO_2 crossover still need further attention in different reactions.[44,73] MEAs for CO_2RR to gas products display less swelling and durability issues, compared with the process of liquid products such as alcohols. As can be seen in Figure 3B, they are difficult owing to the poor faraday efficiency of the liquid products and the product crossover to the anode by the electromigration for anions (such as formate) and electroosmotic flow for the alcohols. Also, the requirement of sufficient CO_2 and water supply will consequently dilute the liquid products.[89,101]

MEA-type CO_2RR can employ three types of ion-change membranes: cation (or proton) exchange membranes, AEMs, and bipolar membranes. Ion transport pathways between the anode and cathode sides are different for each membrane, which can affect CO_2RR efficiency and selectivity. The role of ion-selective membranes in water electrolysis is well studied[110]; however, similar studies have yet to be conducted on CO_2RR and examine parameters such as functional groups concentrations in ion-exchange membranes and ionic conductivity. Particularly, unlike water electrolysis, CO_2RR has several products, and, therefore, the effect of ion-exchange membrane design on the product selectivity needs to be explored for selective formation of the desired products. Regarding the membrane type, CEMs application is limited due to severe HER in the acidic environment of the cathode side. BPMs also possess large membrane potential, leading to a higher required voltage to drive electrolysis and reducing overall energy efficiency.[93] It has been clear that AEMs are the future of MEA-type systems, as their advantages (low HER and high selectivity/energy efficiency) outweigh their disadvantages (mainly CO_2 crossover to anodic side).[72] This calls for the development of advanced AEMs with metrics such as (1) low electrical resistance and high OH^- conductivity, (2) 50%–80% water uptake with lower than 10% swelling, (3) minimal gas/liquid crossover (<0.2%), (4) stability in alkaline (pH: 10–14) and insoluble in 10 wt % alcohol.[72] Meeting all of these metrics sounds complicated, as changing one may alter others, so, therefore, a trade-off needs to be set. Furthermore, the effect of bulk and surface functional groups of the membranes on the local reaction environment and CO_2RR selectivity/efficiency is of great importance. For instance, modulation of pH via incorporation of pyridinium functional groups on the membrane surface resulted in more selective CO_2RR.[106] Similar parameters on the effect of electrolyte have been widely studied,[111] and, thus, more attention needs to be paid regarding MEA-type reactors. The modeling results from McCallum et al.[101] suggested the use of a thinner membrane with a high charge to minimize the carbonate crossover. This inevitably leads to the challenges of maintaining strong mechanical stability of the AEMs while reducing the membrane thickness. Therefore, more efforts are required to develop robust and hydroxide conductive membrane.

On the other hand, as with the catalyst selection, the AEM allows the hydroxide ions generated from the cathode to migrate to the anode for a water oxidation reaction, especially when the membrane is sufficiently thin at high current densities. The alkaline environment at the anode, therefore, allows cheap anode catalysts based on Ni, Fe, or Co to survive. In contrast, the CEMs favor the cation conduction in the MEA configuration, meaning that a sufficiently low pH should be maintained at the anode. The cheap anode based on transition metals will become unstable in the acidic environment.

In the design and scale-up of MEA CO_2RR systems, it is challenging to fabricate electrodes with uniform dispersion of the catalyst, ionomers, and other additives. Even the commercial gas diffusion layer has multiple cracks at the microporous layer, which leads to the flooding issue. Such non-uniformity may cause non-uniform catalytic reactions, temperature hot spots during high-rate electrolysis, and the degradation of the electrode performance and long-term stability. Other critical stability issues also require more attention, including catalyst flooding and salt precipitation at the cathode that blocks CO_2 diffusion and diminish product selectivity[47,54] and the degradation of non-precious metal-based anodes (e.g., Ni-based anodes)[81] that lead to degradation of partial current densities. The catalyst flooding is associated with the loss of the optimal wetting conditions at the CL due to electrowetting and induced cleavage of C–F bonds in the PTFE.[112] A lot can be learned from mature fuel cell technology (PEM fuel cells), especially in terms of MEA fabrication/optimization, as MEA preparation for both fuel cells and CO_2RR follow similar steps, although their unique features need to be considered. This is a common issue for all the gas-diffusion electrodes for CO_2 reduction, not only in MEA configuration but also in other flow cells. Salt precipitation due to carbonation and cation crossover from anolyte is a serious issue for MEA in CO_2RR. In addition, for reactor engineering, such as water management in MEA, many studies are done in fuel cells, which are beneficial to CO_2RR progress.[113] However, the materials used for PEM fuel cells may not be suitable for CO_2RR where higher operating voltages and corrosive anolytes are used. Currently, MEA CO_2RR suffers from product(s)/CO_2 crossover via HCO_3^-/CO_3^{2-} anionic species, and it calls for special attention to the design and fabrication of both GDE and the ion-exchange membranes. In addition, fundamental studies on the mechanism of electrocatalytic reactions, formation of catalyst and ion-exchange membrane interface, and hydrogenation in the absence of liquid electrolyte should be done. This can help to understand the factors involved in the production of the desired products. Besides, MEA CO_2RR still has high energy requirements compared with other competitive technologies, such as solid oxide electrolyzers (SOE), which are operated at a lower voltage. Although SOE works at an elevated temperature, its efficiency is reportedly higher than that of MEA electrolyzer.[114] However, SOE commercialization is hindered by lifetime issues and poor scalability of ceramic-based materials;[30] therefore, advanced catalysts to improve the process kinetics and product selectivity have to be developed.

One of the most important roles of MEA in the whole electrolyzer device is allowing the interface of catalyst-gas reactant-electrolyte to be well controlled by a well-designed configuration. With an in-depth understanding of the reaction mechanism by advanced DFT computation, the surface reaction intermediates can be tuned by different types of MEA to determine the reaction pathway to target product(s). For example, it is well known that an MEA can induce a high local OH^- concentration on the surface of the catalyst, which not only inhibits the competing HER but can significantly enhance the selectivity of C_2/C_{2+} products. Importantly, these highly active local OH^- species can promote the interaction of some critical oxygen-bound intermediates (*$OCHCH_2$, *OCH_2CH_3, etc.) to the catalyst surface. Different from some carbon-bound intermediates (*CO, *CO–COH, etc.) that determine the rate

of the reaction (e.g., partial current of one product), these oxygen-bound species work as a selectivity determining intermediate (SDI) to direct the reaction pathway to a specific product (C_2H_4, C_2H_5OH/C_3H_7OH, or C_2H_6).[115] Currently, the adsorption behavior of these oxygen-bound intermediates is still limited in the CO_2RR field, which needs a well-designed MEA to control the local environment of catalyst-electrolytes as well as some advanced *in situ* spectroscopic technologies.

The multiphysics model development over the MEA is mainly based on advances in PEM fuel cells and electrolyzers. The current low-dimensional models can provide general insights into the underlying mechanisms and controlling steps in the MEAs and have demonstrated their effectiveness for predicting the MEA's performance and potential issues. However, the models at the current stage are limited by insufficient data input of the membrane properties (such as electro-osmotic coefficients), unknown locations and chemistry at the catalyst-ionomer interfaces, and the pore structures at the CLs. This means that more experimental and theoretical efforts are required to obtain properties of the membranes, ionomer-catalyst interfaces, and GDE structures to feed future MEA models. A multiscale model with molecular dynamics considered is another future direction that could provide a more in-depth understanding of the MEA property-performance (i.e., reactivity, selectivity, and stability) relations.

Finally, this review mainly focused on MEAs fabrication for CO_2RR. Furthermore, MEA reactors can be employed for other electrochemical reactions, such as CO or N_2 reductions, which are substantially important reactions toward decentralized fuel/chemical production. Both of these electrochemical reactions have attracted much attention recently for the formation of C_{2+} products and ammonia, respectively.[116,117] A handful of studies on MEA electrolyzers for CO/N_2 are carried out and because ion crossover is not an issue for them, MEA systems can be promising. Although, the production of liquid products (e.g., alcohols or ammonia) via MEA reactors may lead to swelling of the MEA and instability of the electrolyzer.[21] Therefore, more studies are required to take the unique features of these reactions into consideration for high-rate electrolysis.

ACKNOWLEDGMENTS

We acknowledge financial support by University of Southern Queensland (USQ) and Australian Research Council linkage project LP160101729.

AUTHOR CONTRIBUTIONS

Conceptualization, L.G. and H.W.; writing–original draft, L.G., H.R., and M.L.; writing–review & editing, L.G., H.R., M.L., S.S., Y.Z., J.H.L, T.B., and H.W.; supervision, H.W.

REFERENCES

1. Chu, S., and Majumdar, A. (2012). Opportunities and challenges for a sustainable energy future. Nature *488*, 294–303.

2. Lackner, K.S. (2003). Climate change. A guide to CO2 sequestration. Science *300*, 1677–1678.

3. Otto, A., Grube, T., Schiebahn, S., and Stolten, D. (2015). Closing the loop: captured CO2 as a feedstock in the chemical industry. Energy Environ. Sci. *8*, 3283–3297.

4. Müller, L.J., Kätelhön, A., Bringezu, S., McCoy, S., Suh, S., Edwards, R., Sick, V., Kaiser, S., Cuéllar-Franca, R., El Khamlichi, A., et al. (2020). The carbon footprint of the carbon feedstock CO2. Energy Environ. Sci. *13*, 2979–2992.

5. Chen, J.G., Crooks, R.M., Seefeldt, L.C., Bren, K.L., Bullock, R.M., Darensbourg, M.Y., Holland, P.L., Hoffman, B., Janik, M.J., Jones, A.K., et al. (2018). Beyond fossil fuel-driven nitrogen transformations. Science *360*, eaar6611.

6. Sharifian, R., Wagterveld, R.M., Digdaya, I.A., Xiang, C., and Vermaas, D.A. (2021). Electrochemical carbon dioxide capture to close the carbon cycle. Energy Environ. Sci. *14*, 781–814.

7. Service, R.F. (2018). Ammonia—a renewable fuel made from sun, air, and water—could power the globe without carbon. Science *12*, July. 2018, aau7489. https://www.science.org/content/article/ammonia-renewable-fuel-made-sun-air-and-water-could-power-globe-without-carbon.

8. Sun, Z., Ma, T., Tao, H., Fan, Q., and Han, B. (2017). Fundamentals and challenges of electrochemical CO2 reduction using two-dimensional materials. Chem *3*, 560–587.

9. Hu, F., Abeyweera, S.C., Yu, J., Zhang, D., Wang, Y., Yan, Q., and Sun, Y. (2020). Quantifying electrocatalytic reduction of CO2 on twin boundaries. Chem *6*, 3007–3021.

10. Veenstra, F.L.P., Ackerl, N., Martín, A.J., and Pérez-Ramírez, J. (2020). Laser-microstructured copper reveals selectivity patterns in the electrocatalytic reduction of CO2. Chem *6*, 1707–1722.

11. Zhang, X., Liu, Y., Zhang, M., Yu, T., Chen, B., Xu, Y., Crocker, M., Zhu, X., Zhu, Y., Wang, R., et al. (2020). Synergy between β-Mo2C nanorods and non-thermal plasma for selective CO2 reduction to CO. Chem *6*, 3312–3328.

12. Liu, C., Wu, Y., Sun, K., Fang, J., Huang, A., Pan, Y., Cheong, W.-C., Zhuang, Z., Zhuang, Z., Yuan, Q., et al. (2021). Constructing FeN4/graphitic nitrogen atomic interface for high-efficiency electrochemical CO2 reduction over a broad potential window. Chem *7*, 1297–1307.

13. Zhu, C., Zhang, Z., Zhong, L., Hsu, C.-S., Xu, X., Li, Y., Zhao, S., Chen, S., Yu, J., Chen, S., et al. (2021). Product-specific active site motifs of Cu for electrochemical CO2 reduction. Chem *7*, 406–420.

14. Naims, H. (2016). Economics of carbon dioxide capture and utilization—a supply and demand perspective. Environ. Sci. Pollut. Res. Int. *23*, 22226–22241.

15. Delacourt, C., Ridgway, P.L., Kerr, J.B., and Newman, J. (2008). Design of an electrochemical cell making syngas (CO+H2) from CO2and H2O reduction atroom temperature. J.Electrochem .Soc. *155*, B42–B49.

16. Yang, H.B., Hung, S.-F., Liu, S., Yuan, K., Miao, S., Zhang, L., Huang, X., Wang, H.-Y., Cai, W., Chen, R., et al. (2018). Atomically dispersed Ni(I) as the active site for electrochemical CO2 reduction. Nat. Energy *3*, 140–147.

17. Rosen, B.A., Salehi-Khojin, A., Thorson, M.R., Zhu, W., Whipple, D.T., Kenis, P.J.A., and Masel, R.I. (2011). Ionic liquid-mediated selective conversion of CO2 to CO at low overpotentials. Science *334*, 643–644.

18. Smieja, J.M., Sampson, M.D., Grice, K.A., Benson, E.E., Froehlich, J.D., and Kubiak, C.P. (2013). Manganese as a substitute for rhenium in CO2 reduction catalysts: the importance of acids. Inorg. Chem. *52*, 2484–2491.

19. Garg, S., Li, M.R., Weber, A.Z., Ge, L., Li, L.Y., Rudolph, V., Wang, G.X., and Rufford, T.E. (2020). Advances and challenges in electrochemical CO2 reduction processes: an engineering and design perspective looking beyond new catalyst materials. J. Mater. Chem. A *8*, 1511–1544.

20. Sonoyama, N., Kirii, M., and Sakata, T. (1999). Electrochemical reduction of CO2 at metal-porphyrin supported gas diffusion electrodes under high pressure CO2. Electrochem. Commun. *1*, 213–216.

21. Rabiee, H., Ge, L., Zhang, X., Hu, S., Li, M., and Yuan, Z. (2021). Gas diffusion electrodes (GDEs) for electrochemical reduction of carbon dioxide, carbon monoxide, and dinitrogen to value-added products: a review. Energy Environ. Sci. *14*, 1959–2008.

22. Li, M.R., Idros, M.N., Wu, Y.M., Garg, S., Gao, S., Lin, R.J., Rabiee, H., Li, Z.H., Ge, L., Rufford, T.E., et al. (2021). Unveiling the effects of dimensionality of tin oxide-derived catalysts on CO2 reduction by using gas-diffusion electrodes. React. Chem. Eng. *6*, 345–352.

23. Burdyny, T., and Smith, W.A. (2019). CO2 reduction on gas-diffusion electrodes and why catalytic performance must be assessed at commercially-relevant conditions. Energy Environ. Sci. *12*, 1442–1453.

24. Weng, L.C., Bell, A.T., and Weber, A.Z. (2018). Modeling gas-diffusion electrodes for CO2 reduction. Phys. Chem. Chem. Phys. *20*, 16973–16984.

25. Ikeda, S., Ito, T., Azuma, K., Ito, K., and Noda, H. (1995). Electrochemical mass reduction of carbon-dioxide using Cu-loaded gas-diffusion electrodes. 1. Preparation of electrode and reduction products. Denki Kagaku *63*, 303–309.

26. Rabiee, H., Zhang, X., Ge, L., Hu, S., Li, M., Smart, S., Zhu, Z., and Yuan, Z. (2020). Tuning the product selectivity of Cu hollow fiber gas diffusion electrode for efficient CO2 reduction to formate by controlled surface Sn electrodeposition. ACS Appl. Mater. Interfaces *12*, 21670–21681.

27. Rabiee, H., Ge, L., Zhang, X., Hu, S., Li, M., Smart, S., Zhu, Z., and Yuan, Z. (2021). Shape-tuned electrodeposition of bismuth-based nanosheets on flow-through hollow fiber gas diffusion electrode for high-efficiency CO2 reduction to formate. Appl. Catal. B *286*, 119945.

28. Rabiee, H., Ge, L., Zhang, X., Hu, S., Li, M., Smart, S., Zhu, Z., Wang, H., and Yuan, Z. (2021). Stand-alone asymmetric hollow fiber gas-diffusion electrodes with distinguished bronze phases for high-efficiency CO2 electrochemical reduction. Appl. Catal. B *298*, 120538.

29. Lee, W., Kim, Y.E., Youn, M.H., Jeong, S.K., and Park, K.T. (2018). Catholyte-free electrocatalytic CO2 reduction to formate. Angew. Chem. Int. Ed. Engl. *57*, 6883–6887.

30. Ju, H., Kaur, G., Kulkarni, A.P., and Giddey, S. (2019). Challenges and trends in developing technology for electrochemically reducing CO2 in solid polymer electrolyte membrane reactors. J. CO2 Util. *32*, 178–186.

31. Yin, Z., Peng, H., Wei, X., Zhou, H., Gong, J., Huai, M., Xiao, L., Wang, G., Lu, J., and Zhuang, L. (2019). An alkaline polymer electrolyte CO2 electrolyzer operated with pure water. Energy Environ. Sci. *12*, 2455–2462.

32. Weng, L.-C., Bell, A.T., and Weber, A.Z. (2019). Towards membrane-electrode assembly systems for CO2 reduction: a modeling study. Energy Environ. Sci. *12*, 1950–1968.

33. Verma, S., Lu, X., Ma, S., Masel, R.I., and Kenis, P.J.A. (2016). The effect of electrolyte composition on the electroreduction of CO2 to CO on Ag based gas diffusion electrodes. Phys. Chem. Chem. Phys. *18*, 7075–7084.

34. de Tacconi, N.R., Chanmanee, W., Dennis, B.H., and Rajeshwar, K. (2017). Composite copper oxide–copper bromide films for the selective electroreduction of carbon dioxide. J. Mater. Res. *32*, 1727–1734.

35. Dinh, C.T., Burdyny, T., Kibria, M.G., Seifitokaldani, A., Gabardo, C.M., García de Arquer, F.P., Kiani, A., Edwards, J.P., De Luna, P., Bushuyev, O.S., et al. (2018). CO2 electroreduction to ethylene via hydroxide-mediated copper catalysis at an abrupt interface. Science *360*, 783–787.

36. Li, M., Garg, S., Chang, X., Ge, L., Li, L., Konarova, M., Rufford, T.E., Rudolph, V., and Wang, G. (2020). Toward excellence of transition metal-based catalysts for CO2 electrochemical reduction: an overview of strategies and rationales. Small Methods *4*, 2000033.

37. Nitopi, S., Bertheussen, E., Scott, S.B., Liu, X., Engstfeld, A.K., Horch, S., Seger, B., Stephens, I.E.L., Chan, K., Hahn, C., et al. (2019). Progress and perspectives of electrochemical CO2 reduction on copper in aqueous electrolyte. Chem. Rev. *119*, 7610–7672.

38. Fan, L., Xia, C., Yang, F., Wang, J., Wang, H., and Lu, Y. (2020). Strategies in catalysts and electrolyzer design for electrochemical CO2 reduction toward C2+ products. Sci. Adv. *6*, eaay3111.

39. Nguyen, T.N., and Dinh, C.-T. (2020). Gas diffusion electrode design for electrochemical carbon dioxide reduction. Chem. Soc. Rev. *49*, 7488–7504.

40. Malkhandi, S., and Yeo, B.S. (2019). Electrochemical conversion of carbon dioxide to high value chemicals using gas-diffusion electrodes. Curr. Opin. Chem. Eng. *26*, 112–121.

41. Junge Puring, K., Siegmund, D., Timm, J., Möllenbruck, F., Schemme, S., Marschall, R., and Apfel, U.-P. (2021). Electrochemical CO2 reduction: tailoring catalyst layers in gas diffusion electrodes. Adv. Sustain. Syst. *5*, 2000088.

42. Lee, J.-H., Lim, J., Roh, C.-W., Whang, H.S., and Lee, H. (2019). Electrochemical CO2 reduction using alkaline membrane electrode assembly on various metal electrodes. J. CO2 Util. *31*, 244–250.

43. Gabardo, C.M., O'Brien, C.P., Edwards, J.P., McCallum, C., Xu, Y., Dinh, C.-T., Li, J., Sargent, E.H., and Sinton, D. (2019). Continuous carbon dioxide electroreduction to concentrated multi-carbon products using a membrane electrode assembly. Joule *3*, 2777–2791.

44. Larrazábal, G.O., Strøm-Hansen, P., Heli, J.P., Zeiter, K., Therkildsen, K.T., Chorkendorff, I., and Seger, B. (2019). Analysis of mass flows and membrane cross-over in CO2 reduction at high current densities in an MEA-type electrolyzer. ACS Appl. Mater. Interfaces *11*, 41281–41288.

45. Fujinuma, N., Ikoma, A., and Lofland, S.E. (2020). Highly efficient electrochemical CO2 reduction reaction to CO with one-pot synthesized Co-pyridine-derived catalyst

incorporated in a Nafion-based membrane electrode assembly. Adv. Energy Mater. *10*, 2001645.

46. Lee, W.H., Ko, Y.-J., Choi, Y., Lee, S.Y., Choi, C.H., Hwang, Y.J., Min, B.K., Strasser, P., and Oh, H.-S. (2020). Highly selective and scalable CO2 to CO—electrolysis using coral-nanostructured Ag catalysts in zero-gap configuration. Nano Energy *76*, 105030. https://doi.org/10.1016/j.nanoen.2020.105030.

47. Endrődi, B., Kecsenovity, E., Samu, A., Darvas, F., Jones, R.V., Török, V., Danyi, A., and Janáky, C. (2019). Multilayer electrolyzer stack converts carbon dioxide to gas products at high pressure with high efficiency. ACS Energy Lett *4*, 1770–1777.

48. Ham, Y.S., Park, Y.S., Jo, A., Jang, J.H., Kim, S.-K., and Kim, J.J. (2019). Proton-exchange membrane CO2 electrolyzer for CO production using Ag catalyst directly electrodeposited onto gas diffusion layer. J. Power Sources *437*, 226898.

49. Kutz, R.B., Chen, Q., Yang, H., Sajjad, S.D., Liu, Z., and Masel, I.R. (2017). Sustainion imidazolium-functionalized polymers for carbon dioxide electrolysis. Energy Technol *5*, 929–936.

50. Sato, M., Ogihara, H., and Yamanaka, I. (2019). Electrocatalytic reduction of CO2 to CO and CH4 by Co–N–C catalyst and Ni co-catalyst with PEM reactor. ISIJ Int *59*, 623–627.

51. Ogihara, H., Maezuru, T., Ogishima, Y., Inami, Y., Saito, M., Iguchi, S., and Yamanaka, I. (2020). The active center of Co–N–C electrocatalysts for the selective reduction of CO2 to CO using a Nafion-H electrolyte in the gas phase. ACS Omega *5*, 19453–19463.

52. Oh, S., Park, Y.S., Park, H., Kim, H., Jang, J.H., Choi, I., and Kim, S.-K. (2020). Ag-deposited Ti gas diffusion electrode in proton exchange membrane CO2 electrolyzer for CO production. J. Ind. Eng. Chem. *82*, 374–382.

53. Liu, Z., Yang, H., Kutz, R., and Masel, R.I. (2018). CO2 electrolysis to CO and O2 at high selectivity, stability and efficiency using sustainion membranes. J. Electrochem. Soc. *165*, J3371–J3377.

54. Xu, Y., Edwards, J.P., Liu, S., Miao, R.K., Huang, J.E., Gabardo, C.M., O'Brien, C.P., Li, J., Sargent, E.H., and Sinton, D. (2021). Self-cleaning CO2 reduction systems: unsteady electrochemical forcing enables stability. ACS Energy Lett *6*, 809–815.

55. Hou, P., Wang, X., and Kang, P. (2021). Membrane-electrode assembly electrolysis of CO2 to formate using indium nitride nanomaterials. J. CO2 Util. *45*, 2411–2502.

56. Díaz-Sainz, G., Alvarez-Guerra, M., Ávila-Bolívar, B., Solla-Gullón, J., Montiel, V., and Irabien, A. (2021). Improving trade-offs in the figures of merit of gas-phase single-pass continuous CO2 electrocatalytic reduction to formate. Chem. Eng. J. *405*, 126965.

57. de Jesus Gálvez-Vázquez, M., Moreno-García, P., Xu, H., Hou, Y., Hu, H., Montiel, I.Z., Rudnev, A.V., Alinejad, S., Grozovski, V., Wiley, B.J., et al. (2020). Environment matters: CO2RR electrocatalyst performance testing in a gas-fed zero-gap electrolyzer. ACS Catal *10*, 13096–13108.

58. Digdaya, I.A., Sullivan, I., Lin, M., Han, L., Cheng, W.-H., Atwater, H.A., and Xiang, C. (2020). A direct coupled electrochemical system for capture and conversion of CO2 from oceanwater. Nat. Commun. *11*, 4412.

59. Sisler, J., Khan, S., Ip, A.H., Schreiber, M.W., Jaffer, S.A., Bobicki, E.R., Dinh, C.-T., and Sargent, E.H. (2021). Ethylene electrosynthesis: a comparative techno-economic analysis of alkaline vs membrane electrode assembly vs CO2–CO–C2H4 tandems. ACS Energy Lett *6*, 997–1002.

60. Sebastián, D., Palella, A., Baglio, V., Spadaro, L., Siracusano, S., Negro, P., Niccoli, F., and Aricò, A.S. (2017). CO2 reduction to alcohols in a polymer electrolyte membrane co-electrolysis cell operating at low potentials. Electrochim. Acta *241*, 28–40.

61. Gu, Z., Shen, H., Chen, Z., Yang, Y., Yang, C., Ji, Y., Wang, Y., Zhu, C., Liu, J., Li, J., et al. (2021). Efficient electrocatalytic CO2 reduction to C2+ alcohols at defect-site-rich Cu surface. Joule *5*, 429–440.

62. Ogihara, H., Maezuru, T., Ogishima, Y., and Yamanaka, I. (2016). Electrochemical reduction of CO2 to CO by a Co–N–C electrocatalyst and PEM reactor at ambient conditions. ChemistrySelect *1*, 5533–5537.

63. Yan, Z., Hitt, J.L., Zeng, Z., Hickner, M.A., and Mallouk, T.E. (2021). Improving the efficiency of CO2 electrolysis by using a bipolar membrane with a weak-acid cation exchange layer. Nat. Chem. *13*, 33–40.

64. Yang, H.Z., Kaczur, J.J., Sajjad, S.D., and Masel, R.I. (2017). Electrochemical conversion of CO2 to formic acid utilizing Sustainion™ membranes. J. CO2 Util. *20*, 208–217.

65. Díaz-Sainz, G., Alvarez-Guerra, M., Solla-Gullón, J., García-Cruz, L., Montiel, V., and Irabien, A. (2020). Catalyst coated membrane electrodes for the gas phase CO2 electroreduction to formate. Catal. Today *346*, 58–64.

66. Chen, Y., Vise, A., Klein, W.E., Cetinbas, F.C., Myers, D.J., Smith, W.A., Deutsch, T.G., and Neyerlin, K.C. (2020). A robust, scalable platform for the electrochemical conversion of CO2 to formate: identifying pathways to higher energy efficiencies. ACS Energy Lett *5*, 1825–1833.

67. Fan, L., Xia, C., Zhu, P., Lu, Y., and Wang, H. (2020). Electrochemical CO2 reduction to high-concentration pure formic acid solutions in an all-solid-state reactor. Nat. Commun. *11*, 3633.

68. Xia, C., Zhu, P., Jiang, Q., Pan, Y., Liang, W., Stavitski, E., Alshareef, H.N., and Wang, H. (2019). Continuous production of pure liquid fuel solutions via electrocatalytic CO2 reduction using solid-electrolyte devices. Nat. Energy *4*, 776–785.

69. Kaczur, J.J., Yang, H., Liu, Z., Sajjad, S.D., and Masel, R.I. (2018). Carbon dioxide and water electrolysis using new alkaline stable anion membranes. Front. Chem. *6*, 263.

70. Ma, Z., Legrand, U., Pahija, E., Tavares, J.R., and Boffito, D.C. (2021). From CO2 to formic acid fuel cells. Ind. Eng. Chem. Res. *60*, 803–815.

71. Vennekoetter, J.B., Sengpiel, R., and Wessling, M. (2019). Beyond the catalyst: how electrode and reactor design determine the product spectrum during electrochemical CO2 reduction. Chem. Eng. J. *364*, 89–101.

72. Salvatore, D.A., Gabardo, C.M., Reyes, A., O'Brien, C.P., Holdcroft, S., Pintauro, P., Bahar, B., Hickner, M., Bae, C., Sinton, D., et al. (2021). Designing anion exchange membranes for CO2 electrolysers. Nat. Energy *6*, 339–348.

73. Pătru, A., Binninger, T., Pribyl, B., and Schmidt, T.J. (2019). Design principles of bipolar electrochemical co-electrolysis cells for efficient reduction of carbon dioxide from gas phase at low temperature. J. Electrochem. Soc. *166*, F34–F43.

74. Zhang, J., Luo, W., and Züttel, A. (2020). Crossover of liquid products from electrochemical CO2 reduction through gas diffusion electrode and anion exchange membrane. J. Catal. *385*, 140–145.

75. Ma, M., Kim, S., Chorkendorff, I., and Seger, B. (2020). Role of ion-selective membranes in the carbon balance for CO2 electroreduction via gas diffusion electrode reactor designs. Chem. Sci. *11*, 8854–8861.

76. Ma, M., Clark, E.L., Therkildsen, K.T., Dalsgaard, S., Chorkendorff, I., and Seger, B. (2020). Insights into the carbon balance for CO2 electroreduction on Cu using gas diffusion electrode reactor designs. Energy Environ. Sci. *13*, 977–985.

77. Wang, N., Miao, R.K., Lee, G., Vomiero, A., Sinton, D., Ip, A.H., Liang, H., and Sargent, E.H. (2021). Suppressing the liquid product crossover in electrochemical CO2 reduction. SmartMat *2*, 12–16.

78. Krödel, M., Carter, B.M., Rall, D., Lohaus, J., Wessling, M., and Miller, D.J. (2020). Rational design of ion exchange membrane material properties limits the crossover of CO2 reduction products in artificial photosynthesis devices. ACS Appl. Mater. Interfaces *12*, 12030–12042.

79. Ozden, A., Wang, Y., Li, F., Luo, M., Sisler, J., Thevenon, A., Rosas-Hernández, A., Burdyny, T., Lum, Y., Yadegari, H., et al. (2021). Cascade CO2 electroreduction enables efficient carbonate-free production of ethylene. Joule *5*, 706–719.

80. Huang, J.E., Li, F., Ozden, A., Sedighian Rasouli, A., García de Arquer, F.P., Liu, S., Zhang, S., Luo, M., Wang, X., Lum, Y., et al. (2021). CO2 electrolysis to multicarbon products in strong acid. Science *372*, 1074–1078.

81. Vass, Á., Endrődi, B., Samu, G.F., Balog, Á., Kormányos, A., Cherevko, S., and Janáky, C. (2021). Local chemical environment governs anode processes in CO2 electrolyzers. ACS Energy Lett *6*, 3801–3808.

82. Pärnamäe, R., Mareev, S., Nikonenko, V., Melnikov, S., Sheldeshov, N., Zabolotskii, V., Hamelers, H.V.M., and Tedesco, M. (2021). Bipolar membranes: a review on principles, latest developments, and applications. J. Membr. Sci. *617*, 118538.

83. Li, Y.C., Zhou, D., Yan, Z., Gonçalves, R.H., Salvatore, D.A., Berlinguette, C.P., and

Mallouk, T.E. (2016). Electrolysis of CO2 to syngas in bipolar membrane-based electrochemical cells. ACS Energy Lett *1*, 1149–1153.

84. Pan, J., Lu, S., Li, Y., Huang, A., Zhuang, L., and Lu, J. (2010). High-performance alkaline polymer electrolyte for fuel cell applications. Adv. Funct. Mater. *20*, 312–319.

85. Reyes, A., Jansonius, R.P., Mowbray, B.A.W., Cao, Y., Wheeler, D.G., Chau, J., Dvorak, D.J., and Berlinguette, C.P. (2020). Managing hydration at the cathode enables efficient CO2 electrolysis at commercially relevant current densities. ACS Energy Lett *5*, 1612–1618.

86. Shafaque, H.W., Lee, C., Fahy, K.F., Lee, J.K., LaManna, J.M., Baltic, E., Hussey, D.S., Jacobson, D.L., and Bazylak, A. (2020). Boosting membrane hydration for high current densities in membrane electrode assembly CO2 electrolysis. ACS Appl. Mater. Interfaces *12*, 54585–54595.

87. Leonard, M.E., Clarke, L.E., Forner-Cuenca, A., Brown, S.M., and Brushett, F.R. (2020). Investigating electrode flooding in a flowing electrolyte, gas-fed carbon dioxide electrolyzer. ChemSusChem *13*, 400–411.

88. Endrődi, B., Kecsenovity, E., Samu, A., Halmágyi, T., Rojas-Carbonell, S., Wang, L., Yan, Y., and Janáky, C. (2020). High carbonate ion conductance of a robust PiperION membrane allows industrial current density and conversion in a zero-gap carbon dioxide electrolyzer cell. Energy Environ. Sci. *13*, 4098–4105.

89. Wheeler, D.G., Mowbray, B.A.W., Reyes, A., Habibzadeh, F., He, J., and Berlinguette, C.P. (2020). Quantification of water transport in a CO2 electrolyzer. Energy Environ. Sci. *13*, 5126–5134.

90. Endrődi, B., Samu, A., Kecsenovity, E., Halmágyi, T., Sebők, D., and Janáky, C. (2021). Operando cathode activation with alkali metal cations for high current density operation of water-fed zero-gap carbon dioxide electrolyzers. Nat. Energy *6*, 439–448.

91. Verma, S., Hamasaki, Y., Kim, C., Huang, W., Lu, S., Jhong, H.-R.M., Gewirth, A.A., Fujigaya, T., Nakashima, N., and Kenis, P.J.A. (2018). Insights into the low overpotential electroreduction of CO2 to CO on a supported gold catalyst in an alkaline flow electrolyzer. ACS Energy Lett *3*, 193–198.

92. Salvatore, D., and Berlinguette, C.P. (2020). Voltage matters when reducing CO2 in an electrochemical flow cell. ACS Energy Lett *5*, 215–220.

93. Vargas-Barbosa, N.M., Geise, G.M., Hickner, M.A., and Mallouk, T.E. (2014). Assessing the utility of bipolar membranes for use in photoelectrochemical water-splitting cells. ChemSusChem *7*, 3017–3020.

94. O'Brien, C.P., Miao, R.K., Liu, S., Xu, Y., Lee, G., Robb, A., Huang, J.E., Xie, K., Bertens, K., Gabardo, C.M., et al. (2021). Single pass CO2 conversion exceeding 85% in the electrosynthesis of multicarbon products via local CO2 regeneration. ACS Energy Lett *6*, 2952–2959.

95. Miao, R.K., Xu, Y., Ozden, A., Robb, A., O'Brien, C.P., Gabardo, C.M., Lee, G., Edwards, J.P., Huang, J.E., Fan, M., et al. (2021). Electroosmotic flow steers neutral products and enables concentrated ethanol electroproduction from CO2. Joule *5*, 2742–2753.

96. Weber, A.Z., Borup, R.L., Darling, R.M., Das, P.K., Dursch, T.J., Gu, W., Harvey, D., Kusoglu, A., Litster, S., Mench, M.M., et al. (2014). A critical review of modeling transport phenomena in polymer-electrolyte fuel cells. J. Electrochem. Soc. *161*, F1254–F1299.

97. Kubannek, F., Turek, T., and Krewer, U. (2019). Modeling oxygen gas diffusion electrodes for various technical applications. Chem. Ing. Tech. *91*, 720–733.

98. Olivier, P., Bourasseau, C., and Bouamama, P.B. (2017). Low-temperature electrolysis system modelling: a review. Renew. Sustain. Energ. Rev. *78*, 280–300.

99. Le Bideau, D., Mandin, P., Benbouzid, M., Kim, M., and Sellier, M. (2019). Review of necessary thermophysical properties and their sensivities with temperature and electrolyte mass fractions for alkaline water electrolysis multiphysics modelling. Int. J. Hydrog. Energy *44*, 4553–4569.

100. Falcão, D.S., and Pinto, A.M.F.R. (2020). A review on PEM electrolyzer modelling: guidelines for beginners. J. Clean. Prod. *261*, 121184.

101. McCallum, C., Gabardo, C.M., O'Brien, C.P., Edwards, J.P., Wicks, J., Xu, Y., Sargent, E.H., and Sinton, D. (2021). Reducing the crossover of carbonate and liquid products during carbon dioxide electroreduction. Cell Rep. Physiol. Sci. *2*, 100522.

102. Spry, D.B., and Fayer, M.D. (2009). Proton transfer and proton concentrations in protonated Nafion fuel cell membranes. J. Phys. Chem. B *113*, 10210–10221.

103. Sondheimer, S.J., Bunce, N.J., Lemke, M.E., and Fyfe, C.A. (1986). Acidity and catalytic activity of Nafion-H. Macromolecules *19*, 339–343.

104. Fornaciari, J.C., Gerhardt, M.R., Zhou, J., Regmi, Y.N., Danilovic, N., Bell, A.T., and Weber, A.Z. (2020). The role of water in vapor-fed proton-exchange-membrane electrolysis. J. Electrochem. Soc. *167*, 104508.

105. Weng, L.-C., Bell, A.T., and Weber, A.Z. (2020). A systematic analysis of Cu-based membrane-electrode assemblies for CO2 reduction through multiphysics simulation. Energy Environ. Sci. *13*, 3592–3606.

106. Ovalle, V.J., and Waegele, M.M. (2019). Understanding the impact of *N*-arylpyridinium ions on the selectivity of CO2 reduction at the Cu/electrolyte interface. J. Phys. Chem. C *123*, 24453–24460.

107. Singh, M.R., Kwon, Y., Lum, Y., Ager, J.W., and Bell, A.T. (2016). Hydrolysis of electrolyte cations enhances the electrochemical reduction of CO2 over Ag and Cu. J. Am. Chem. Soc. *138*, 13006–13012.

108. Subramanian, S., Middelkoop, J., and Burdyny, T. (2021). Spatial reactant distribution in CO2 electrolysis: balancing CO2 utilization and faradaic efficiency. Sustain. Energy Fuels *5*, 6040–6048.

109. Wiley, D., and Fimbres Weihs, G. (2016). Electroosmotic drag in membranes. In Encyclopedia of Membranes, E. Drioli and L. Giorno, eds. (Springer), pp. 653–654. https://doi.org/10.1007/978-3-662-44324-8_2078.

110. Oener, S.Z., Ardo, S., and Boettcher, S.W. (2017). Ionic processes in water electrolysis: the role of ion-selective membranes. ACS Energy Lett *2*, 2625–2634.

111. Sa, Y.J., Lee, C.W., Lee, S.Y., Na, J., Lee, U., and Hwang, Y.J. (2020). Catalyst-electrolyte interface chemistry for electrochemical CO2 reduction. Chem. Soc. Rev. *49*, 6632–6665.

112. Yang, K., Kas, R., Smith, W.A., and Burdyny, T. (2021). Role of the carbon-based gas diffusion layer on flooding in a gas diffusion electrode cell for electrochemical CO2 reduction. ACS Energy Lett *6*, 33–40.

113. Pasaogullari, U., and Wang, C.Y. (2004). Liquid water transport in gas diffusion layer of polymer electrolyte fuel cells. J. Electrochem. Soc. *151*, 399–406.

114. Lo Faro, M., Zignani, S.C., Trocino, S., Antonucci, V., and Aricò, A.S. (2019). New insights on the co-electrolysis of CO2 and H2O through a solid oxide electrolyser operating at intermediate temperatures. Electrochim. Acta *296*, 458–464.

115. Yang, Y., Qiao, S., Zheng, M., Zhou, J., and Quan, X. (2019). Enhanced permeability, contaminants removal and antifouling ability of CNTs-based hollow fiber membranes under electrochemical assistance. J. Membr. Sci. *582*, 335–341.

116. Xu, H., Ithisuphalap, K., Li, Y., Mukherjee, S., Lattimer, J., Soloveichik, G., and Wu, G. (2020). Electrochemical ammonia synthesis through N2 and H2O under ambient conditions: theory, practices, and challenges for catalysts and electrolytes. Nano Energy *69*, 104469. https://doi.org/10.1016/j.nanoen.2020.104469.

117. Jouny, M., Hutchings, G.S., and Jiao, F. (2019). Carbon monoxide electroreduction as an emerging platform for carbon utilization. Nat. Catal. *2*, 1062–1070.